

# Learning Uncertainty-Aware Temporally-Extended Actions

Joongkyu Lee<sup>1\*</sup>, Seung Joon Park<sup>2\*</sup>, Yunhao Tang<sup>3</sup>, Min-hwan Oh<sup>1</sup>

<sup>1</sup>Seoul National University

<sup>2</sup>Samsung Research

<sup>3</sup>Google DeepMind

jklee0717@snu.ac.kr, soonjun.park@samsung.com, robintyh@deepmind.com, minoh@snu.ac.kr

## Abstract

In reinforcement learning, temporal abstraction in the action space, exemplified by action repetition, is a technique to facilitate policy learning through extended actions. However, a primary limitation in previous studies of action repetition is its potential to degrade performance, particularly when sub-optimal actions are repeated. This issue often negates the advantages of action repetition. To address this, we propose a novel algorithm named **Uncertainty-aware Temporal Extension (UTE)**. UTE employs ensemble methods to accurately measure uncertainty during action extension. This feature allows policies to strategically choose between emphasizing exploration or adopting an uncertainty-averse approach, tailored to their specific needs. We demonstrate the effectiveness of UTE through experiments in Gridworld and Atari 2600 environments. Our findings show that UTE outperforms existing action repetition algorithms, effectively mitigating their inherent limitations and significantly enhancing policy learning efficiency.

## Introduction

Temporal abstraction is a promising approach to solving complex tasks in reinforcement learning (RL) with complex structures and long horizons (Fikes, Hart, and Nilsson 1972; Dayan and Hinton 1992; Parr and Russell 1997; Sutton, Precup, and Singh 1999; Precup 2000; Bacon, Harb, and Precup 2017; Barreto et al. 2019; Machado, Barreto, and Precup 2021). Hierarchical reinforcement learning (HRL) enables the decomposition of this sequential decision-making problem into simpler lower-level actions or subtasks. Intuitively, an agent explores the environment more effectively when operating at a higher level of abstraction and solving smaller subtasks (Machado, Barreto, and Precup 2021). One of the most prominent approaches for HRL is the *option* framework (Sutton, Precup, and Singh 1999; Precup 2000), which describes the hierarchical structure in decision making in terms of temporally-extended courses of action. Temporally-extended actions have been shown to speed up learning, potentially providing more effective exploration compared to single-step explorative action and requiring a smaller number of high-level decisions when solving a problem (Stolle

and Precup 2002; Biedenkapp et al. 2021). From a cognitive perspective, such observations are also coherent with how humans learn, generalize from experiences, and perform abstraction over tasks (Xia and Collins 2021).

There has been a line of works that propose repetition of action for an extended period as a specialized form of temporal abstraction (Lakshminarayanan, Sharma, and Ravindran 2017; Sharma, Srinivas, and Ravindran 2017; Dabney, Ostrovski, and Barreto 2020; Metelli et al. 2020; Biedenkapp et al. 2021; Park, Kim, and Kim 2021).<sup>1</sup> Hence, the action-repetition methods address the problem of learning when to perform a new action while repeating an action for multiple time-steps (Dabney, Ostrovski, and Barreto 2020; Biedenkapp et al. 2021). The extension length, the interaction steps to repeat the same action, is learned by an agent along with what action to execute (Sharma, Srinivas, and Ravindran 2017; Biedenkapp et al. 2021). As shown by the improved empirical performances (Dabney, Ostrovski, and Barreto 2020; Biedenkapp et al. 2021), these action repetition approaches can be well justified by the *commitment* to action for deriving a deeper exploration. These approaches can help suppress the dithering behavior of the agent that can result in short-sighted exploration in a local neighborhood.

However, simple action repetition alone cannot guarantee performance improvement. Repetition of a sub-optimal action for an extended period can lead to severe deterioration in the performance. For example, a game may terminate due to reckless action repetition when an agent is in a dangerous region. A more uncertainty-averse behavior would be helpful in this scenario. On the other hand, an agent may linger in the local neighborhood due to a lack of optimism, especially in sparse reward settings. In that case, a more exploration-favor behavior can be beneficial. In either case, a suitable control of uncertainty of value estimates over longer horizons can be a crucial element. In particular, the calibration of how much exploration the agent can take, or how uncertainty-averse the agent should be, can definitely depend on an environment. Thus, the degree of uncertainty to be considered should be

<sup>1</sup>In fact, action repetition for a fixed number of steps was one of the strategies deployed in solving Atari 2600 games (Mnih et al. 2015; Machado et al. 2018). Despite its simplicity, the action repetition provided sufficient performance gains so that almost all modern methods of solving Atari games are still implementing such action repetitions.

\*These authors contributed equally.

adaptive depending on the environment. To this end, we propose to account for uncertainties when repeating actions. To our best knowledge, consideration of uncertainty in the future when instantiating action repetition has been not addressed previously. Such consideration is essential in action repetition in both uncertainty-averse and exploration-favor environments.

In this paper, we propose a novel method that learns to repeat actions while incorporating the estimated uncertainty of the repeated action values. We can either impose aggressive or uncertainty-averse exploration by controlling the degree of uncertainty in order to take suitable uncertainty-aware strategy for the environment. Through extensive experiments and ablation studies, we demonstrate the efficacy of our proposed method and how it enhances the performances of deep reinforcement learning agents in various environments. In comparison with the benchmarks, we show that our proposed method outperforms baselines, consistently outperforming the existing action repetition methods. Our contributions are:

- We present a novel framework that allows the agent to repeat actions in a uncertainty-aware manner using an ensemble method. Suitably controlling the amount of uncertainty induced by repeated actions, our proposed method learns to choose extension length and learns how *optimistic* or *pessimistic* it should be, hence enabling efficient exploration.
- Our method yields a salient insight that it is beneficial to consider environment-inherent uncertainty preference. Some environments are uncertainty-favor (Chain MDP), and some are uncertainty-averse (Gridworlds).
- In a set of testing environments, we show UTE consistently outperforms all of the existing action-repetition baselines, such as DAR,  $\epsilon z$ -Greedy, DQN, B-DQN, in terms of final evaluation scores, learning speed, and coverage of state-spaces.

## Related Work

**Temporal Abstraction and Action Repetition.** Temporal abstractions can be viewed as an attempt to find a time scale that is adequate for describing the actions of an AI system (Precup 2000). The options framework (Sutton, Precup, and Singh 1999; Precup 2000; Bacon, Harb, and Precup 2017) formalizes the idea of temporally-extended actions. An MDP endowed with a set of options are called Semi-Markov Decision Process (SMDP) which we define in Preliminaries. The generalization of conventional action-value functions for the options framework is called *option*-value functions (Sutton, Precup, and Singh 1999). The mapping from states to probabilities of taking an option is called policy over options. In the options framework, the agent attempts to learn a policy over options that maximizes the option-value functions.

One simple form of an option is repeating a primitive action for certain number of steps (Schoknecht and Riedmiller 2002). Action repetition has been widely explored in the literature (Lakshminarayanan, Sharma, and Ravindran 2017; Sharma, Srinivas, and Ravindran 2017; Dabney, Ostrovski, and Barreto 2020; Metelli et al. 2020; Biedenkapp et al. 2021; Park, Kim, and Kim 2021). Action repetition

has been empirically shown to induce deeper exploration (Dabney, Ostrovski, and Barreto 2020) and lead to efficient learning by reducing the granularity of control (Lakshminarayanan, Sharma, and Ravindran 2017; Sharma, Srinivas, and Ravindran 2017; Metelli et al. 2020; Biedenkapp et al. 2021). Action repetition can be implemented by deciding the extension length of an action which is either sampled from a distribution (Dabney, Ostrovski, and Barreto 2020) or returned by a policy (Lakshminarayanan, Sharma, and Ravindran 2017; Sharma, Srinivas, and Ravindran 2017). The closest related to our work is Biedenkapp et al. (2021). They proposed an algorithm called TempoRL that not only selects an action in a state but also for how long to commit to that action. TempoRL (Biedenkapp et al. 2021) proposes a hierarchical structure in which *behavior* policy determines the action  $a$  to be played given the current state  $s$ , and a *skip* policy determines how long to repeat this action. However, our main intuition is that simply repeating the chosen action is not enough. We may encounter undesirable states while repeating the action. This could lead to catastrophic failure when an agent enters a “risky” area (refer Gridworlds experiments). Our method has been shown to effectively manage this issue by quantifying the uncertainty of the option in form of repeating actions.

**Uncertainty in Reinforcement Learning.** Recently, many works have made significant advances in empirical studies by quantifying and incorporating uncertainty (Osband et al. 2016; Bellemare et al. 2016; Badia et al. 2020; Lee et al. 2022). There are two types of uncertainty: aleatoric and epistemic. Aleatoric uncertainty is the uncertainty caused by the uncontrollable stochastic nature of the environment and cannot be reduced. Epistemic uncertainty is caused by the current imperfect training of the neural network and can be reducible.

One mainstream of estimating the uncertainty in deep RL relies on bootstrapping. Osband et al. (2016) introduced Bootstrapped DQN as a method for efficient exploration. This approach is a variation of the classic DQN neural network architecture, which has a shared torso with  $K \in \mathbb{Z}^+$  heads. Anschel, Baram, and Shimkin (2017); Peer et al. (2021) leveraged an ensemble of Q-functions to mitigate overestimation in DQN. In this paper, we propose an algorithm that quantifies uncertainty of Q-value estimates of the states reached under the repeated-action. This algorithm utilizes multiple randomly-initialized bootstrapped heads that stretch out from a shared network, providing multiple estimates of the *option*-value function. The variance between these estimates is then used as a measure of uncertainty. Notably, this approach allows us to capture both aleatoric and epistemic uncertainty. Then, we establish a UCB-style (Auer, Cesa-Bianchi, and Fischer 2002; Audibert, Munos, and Szepesvári 2009) option-selecting algorithm that simply adds the estimated uncertainty to the averaged ensemble Q-values and chooses an action that maximizes the quantity (Chen et al. 2017; Peer et al. 2021).

## Preliminaries and Notations

In reinforcement learning, an agent interacts with an environment whose underlying dynamics is modeled by a Markov Decision Process (MDP) (Puterman 2014). The tuple  $\langle \mathcal{S}, \mathcal{A}, P, R, \gamma \rangle$  defines an MDP  $\mathcal{M}$ , where  $\mathcal{S}$  is a state

space,  $\mathcal{A}$  is an action space,  $P : \mathcal{S} \times \mathcal{A} \rightarrow \mathcal{S}$  is a transition dynamics function,  $r : \mathcal{S} \times \mathcal{A} \rightarrow \mathbb{R}$  is a reward function, and  $\gamma \in [0, 1]$  is the discount factor. We consider a Semi-Markov Decision Process (SMDP) model to incorporate the options framework (Sutton, Precup, and Singh 1999; Precup 2000). An SMDP is an original MDP with a set of options, i.e.,  $\mathcal{M}_o := \langle \mathcal{S}, \Omega, P_o, R_o \rangle$ , where  $\omega \in \Omega$  is an option in the option space,  $P_o(s' | s, \omega) : \mathcal{S} \times \Omega \rightarrow \mathcal{S}$  is the probability of transitioning from state  $s$  to state  $s'$  after taking an option  $\omega$  and  $R_o : \mathcal{S} \times \Omega \rightarrow \mathbb{R}$  is the reward function for the option.

For any set  $\mathcal{X}$ , let  $\mathcal{P}(\mathcal{X})$  denote the space of probability distributions over  $\mathcal{X}$ . Then a policy over option  $\pi_\omega : \mathcal{S} \rightarrow \mathcal{P}(\Omega)$  assigns a probability to an option conditioned on a given state. Our goal is to learn a policy  $\pi_\omega$  that maximizes the expectation of discounted return starting from an initial state  $s_0$ ; then, define the value functions  $V^{\pi_\omega}(s_0) = \mathbb{E}_{\pi_\omega}[\sum_{t=0}^{\infty} \gamma^t R_t | s_0]$ , the action-value functions  $Q^{\pi_\omega}(s_0, a) = \mathbb{E}_{\pi_\omega}[\sum_{t=0}^{\infty} \gamma^t R_t | s_0, a]$ , or the option-value functions  $\tilde{Q}^{\pi_\omega}(s_0, \omega) = \mathbb{E}_{\pi_\omega}[\sum_{t=0}^{\infty} \gamma^t R_t | s_0, \omega]$ .

In general, options depend on the entire *history* between time step  $t$  when they were initiated and the current time step  $t+k$ ,  $h_{t:t+k} := s_t a_t s_{t+1} \dots a_{t+k-1} s_{t+k}$ . Let  $\mathcal{H}$  be the space of all possible histories  $h$ , then a *semi-Markov option*  $\omega$  is a tuple  $\omega := \langle \mathcal{I}_o, \pi_o, \beta_o \rangle$ , where  $\mathcal{I}_o \subset \mathcal{S}$  is an initiation set,  $\pi_o : \mathcal{H} \rightarrow \mathcal{P}(\mathcal{A})$  is an *intra-option* policy, and  $\beta_o : \mathcal{H} \rightarrow [0, 1]$  is a termination function. In this framework, we define an action repeating option to be  $\omega_{a_j} := \langle \mathcal{S}, \mathbf{1}_a, \beta(h) = \mathbf{1}_{|h|=j} \rangle$ , in which  $h \in \mathcal{H}$  and  $\mathbf{1}_a$  indicates  $|\mathcal{A}|$ -dimensional vector where the element corresponding to  $a$  is 1 and 0 otherwise. This action repeating option takes action  $a$  for  $j$  times and then terminates.

When an agent plays a chosen action for extension length  $j$ , total of  $\frac{j(j+1)}{2}$  skip-transitions are observed and stored in the replay buffer (Biedenkapp et al. 2021). Specifically, when repeating the action for  $j$  times from state  $s$ , we can also experience  $(s \rightarrow s'_{(1)})$ ,  $(s \rightarrow s'_{(2)})$ ,  $\dots$ ,  $(s'_{(1)} \rightarrow s'_{(2)})$ ,  $\dots$ ,  $(s'_{(j-1)} \rightarrow s'_{(j)})$ , in total  $\frac{j \cdot (j+1)}{2}$  transitions. We leverage these transitions to update option-values. Consequently, the observations for short extensions are updated more frequently, leading to smaller uncertainties for short extensions and larger uncertainties for long extensions.

## Uncertainty-aware Temporal Extension

In this section, we propose our algorithm UTE: Uncertainty-aware Temporal Extension, which repeats the action in consideration of uncertainty in Q-values. We first demonstrate temporally-extended Q-learning by decomposing the action repeating option. We then describe how we estimate the uncertainty of an option-value function  $\tilde{Q}^{\pi_\omega}$  by utilizing the ensemble method to select an extension length  $j$  in consideration of uncertainty. We additionally show that  $n$ -step targets can be used for learning the action-value function  $Q^{\pi_\omega}$  without worrying about off-policy correction.

## Temporally-extended Q-Learning

In this work, we mainly depend on techniques based on the Q-learning algorithm (Watkins and Dayan 1992), which seeks

---

## Algorithm 1: UTE: Uncertainty-aware Temporal Extension

---

- 1: **Input:** uncertainty parameter  $\lambda$ , the number of output heads of option-value functions  $B$ .
  - 2: **Initialize:**  $Q^{\pi_\omega}, \{\tilde{Q}_{(b)}^{\pi_\omega}\}_{b=1}^B$ .
  - 3: **for** episode = 1,  $\dots$ ,  $K$  **do**
  - 4:   Obtain initial state  $s$  from environment
  - 5:   **repeat**
  - 6:      $a \leftarrow \epsilon$ -greedy  $\operatorname{argmax}_{a'} Q^{\pi_\omega}(s, a)$
  - 7:     Calculate  $\hat{\mu}_{\pi_\omega}(s, \omega_{a_j}), \hat{\sigma}_{\pi_\omega}^2(s, \omega_{a_j})$  by Eq. (4).
  - 8:      $j \leftarrow \operatorname{argmax}_{j'} \{\hat{\mu}_{\pi_\omega}(s, \omega_{a_{j'}}) + \lambda \hat{\sigma}_{\pi_\omega}(s, \omega_{a_{j'}})\}$
  - 9:     **while**  $j \neq 0$  and  $s$  is not terminal **do**
  - 10:       Take action  $a$  and observe  $s', r$
  - 11:        $s \leftarrow s', j \leftarrow j - 1$
  - 12:     **end while**
  - 13:   **until** episode ends
  - 14: **end for**
- 

to approximate the Bellman optimality operator to learn the optimal policy:

**Definition 1.** We define the optimal action-value function  $Q^{\pi_\omega^*}$  and the optimal option-value function  $\tilde{Q}^{\pi_\omega^*}$  respectively as

$$Q^{\pi_\omega^*}(s, a) = \mathbb{E}_{s'_{(1)} \sim P} \left[ R(s, a) + \gamma \max_{a'} Q^{\pi_\omega^*}(s'_{(1)}, a') \right], \quad (1)$$

$$\tilde{Q}^{\pi_\omega^*}(s, \omega_{a_j}) = \mathbb{E}_{s'_{(j)} \sim P_o} \left[ R_o(s, \omega_{a_j}) + \gamma^j \max_{\omega'} \tilde{Q}^{\pi_\omega^*}(s'_{(j)}, \omega') \right], \quad (2)$$

where  $s'_{(0)}$  and  $s'_{(j)}$ , respectively, indicate one-step and  $j$ -step later state from the state  $s$ . In practice, it is common to use a function approximator to estimate each Q-value,  $Q^{\pi_\omega}(s, a; \theta) \approx Q^{\pi_\omega^*}(s, a)$  and  $\tilde{Q}^{\pi_\omega}(s, \omega_{a_j}; \phi) \approx \tilde{Q}^{\pi_\omega^*}(s, \omega_{a_j})$ . We use two different neural network function approximators parameterized by  $\theta$  and  $\phi$  respectively.

**Option Decomposition.** Learning the optimal policy over options, instead of the optimal action policy, has the same effect as enlarging the action space from  $|\mathcal{A}|$  to  $|\mathcal{A}| \times |\mathcal{J}|$ , where  $\mathcal{J} = \{1, 2, \dots, \max \text{repetition}\}$ . Generally, inaccuracies in Q-function estimations can cause the learning process to converge to a sub-optimal policy, and this phenomenon is amplified in situations with large action spaces (Thrun and Schwartz 1993; Zahavy et al. 2018). Therefore, we consider decomposed policy over option (Biedenkapp et al. 2021),  $\pi_\omega(\omega_{a_j} | s) := \pi_a(a | s) \cdot \pi_e(j | s, a)$ , in which an action policy  $\pi_a(a | s) : \mathcal{S} \rightarrow \mathcal{P}(\mathcal{A})$  assigns some probability to each action conditioned on a given state, and then an extension policy  $\pi_e(j | s, a) : \mathcal{S} \times \mathcal{A} \rightarrow \mathcal{P}(\mathcal{J})$  assigns some probability to each extension length conditioned on a given state and action. Note that there exists a hierarchy between decomposed policies  $\pi_a$  and  $\pi_e$ , thus,  $\pi_a$  always has to be queried before  $\pi_e$  at every time an option initiates. The agent first chooses an action  $a$  from action policy  $\pi_a$  based on the action-value function  $Q^{\pi_\omega}$  (e.g.  $\epsilon$ -greedy). Then, given this action  $a$ , it selects extension length  $j$  from  $\pi_e$  according to the option-value function  $\tilde{Q}^{\pi_\omega}$ .

By decomposing the policy over option  $\pi_\omega$ , we can decrease the search space from  $|\mathcal{A}| \times |\mathcal{J}|$  to  $|\mathcal{A}| + |\mathcal{J}|$ . We empirically show that decomposing option can stabilize the Q-learning in Appendix. However, this learning process may converge to a sub-optimal policy because it is intractable to search all the possible combinations of actions and extension lengths  $(a, j)$ . The agent may repeat the sub-optimal action excessively or sometimes be overly myopic. Our algorithm can mitigate this issue by controlling the level of uncertainty when executing the extension policy  $\pi_e$ .

**Proposition 1.** *In a Semi-Markov Decision Process (SMDP), let an option  $\omega \in \Omega$  be the action repeating option defined by action  $a$  and extension length  $j$ , i.e.  $\omega_{aj} := \langle \mathcal{S}, \mathbf{1}_a, \beta(h) = \mathbf{1}_{h=j} \rangle$ . For all  $\omega \in \Omega$ , a policy over option,  $\pi_\omega$ , can be decomposed by an action policy  $\pi_a(a | s) : \mathcal{S} \rightarrow \mathcal{P}(\mathcal{A})$  and an extension policy  $\pi_e(j | s, a) : \mathcal{S} \times \mathcal{A} \rightarrow \mathcal{P}(|\mathcal{J}|)$ , i.e.  $\pi_\omega(\omega_{aj} | s) := \pi_a(a | s) \cdot \pi_e(j | s, a)$ . Then, for the corresponding optimal policy  $\pi_\omega^*$ , the following holds:*

$$V^{\pi_\omega^*}(s) = \max_{\omega_{aj}} Q^{\pi_\omega^*}(s, \omega_{aj}) = \max_a Q^{\pi_\omega^*}(s, a).$$

Proposition 1 implies that the target value for the option selection of repeated actions can be the same as the target for a single-step action selection within the option. In our implementation, we use  $\max_{a'} Q^{\pi_\omega^*}(s'_{(j)}, a')$  instead of  $\max_{\omega'} \tilde{Q}^{\pi_\omega^*}(s'_{(j)}, \omega'_{aj})$  for the target value in Eq.(2). This can stabilize the learning process by sharing the same target.

### Ensemble-based Uncertainty Quantification

In the previous action repetition methods (Lakshminarayanan, Sharma, and Ravindran 2017; Sharma, Srinivas, and Ravindran 2017; Dabney, Ostrovski, and Barreto 2020; Biedenkapp et al. 2021), they extend the chosen action without considering uncertainty which could easily run to failure. The only situation where these problems do not occur is when their extension policies are optimal, which means they need to expect the  $j$  step later state precisely. However, it is improbable in the sense that this situation rarely occurs in the learning process. In order to solve this problem, we propose a strategy of choosing a extension length  $j$  in an uncertainty-aware manner. UTE is a uncertainty-aware version of the TempoRL (Biedenkapp et al. 2021). Our main intuition is that it is crucial to consider the uncertainty of option-value functions  $\tilde{Q}^{\pi_\omega}$ , when selecting extension length  $j$  by extension policy  $\pi_e$ .

We use the ensemble method, which has recently become prevalent in RL (Osband et al. 2016; Da Silva et al. 2020; Bai et al. 2021), to estimate uncertainty in our estimated option-value functions. We use a network consisting of a shared architecture with  $B$  independent. ‘‘head’’ branching off from the shared network. Each head corresponds to a option-value function,  $\tilde{Q}_{(b)}^{\pi_\omega}$ , for  $b \in \{1, 2, \dots, B\}$ . Each head is randomly-initialized and trained by different samples from an experience buffer. Unlike Bootstrapped DQN (B-DQN) (Osband et al. 2016) where each one of the value function heads is trained against its own target network, our UTE trains each value function head against the same target.

If each head has its own target head respectively, since the objective function of neural networks is generally non-convex, each Q-value may converge to different modes. In this case, as training the policy, the estimated uncertainty of option Q-value,  $\hat{\sigma}_{\pi_\omega}$ , could not converge to zero. This means that it is unable to learn an optimal policy. Therefore, using the same target is one of the key points of our implementation.

Given state  $s$  and action  $a$ ,  $\tilde{Q}_{(b)}^{\pi_\omega}$ -values are aggregated by extension length  $j$  to estimate mean and variance as follows:

$$\hat{\mu}_{\pi_\omega}(s, \omega_{aj}) := \frac{1}{B} \sum_{b=1}^B \tilde{Q}_{(b)}^{\pi_\omega}(s, \omega_{aj}) \quad (3)$$

$$\hat{\sigma}_{\pi_\omega}^2(s, \omega_{aj}) := \frac{1}{B} \sum_{b=1}^B (\tilde{Q}_{(b)}^{\pi_\omega}(s, \omega_{aj}))^2 - (\hat{\mu}_{\pi_\omega}(s, \omega_{aj}))^2 \quad (4)$$

Then, we define *uncertainty-aware* extension policy  $\pi_e$ , which takes extension length  $j$  deterministically given state and action, by introducing the uncertainty parameter  $\lambda \in \mathbb{R}$ :

$$j = \operatorname{argmax}_{j' \in \mathcal{J}} \{ \hat{\mu}_{\pi_\omega}(s, \omega_{aj'}) + \lambda \hat{\sigma}_{\pi_\omega}(s, \omega_{aj'}) \}.$$

where  $\lambda$  indicates the level of uncertainty to be considered. The positive  $\lambda$  induces more aggressive exploration, and the negative one causes uncertainty-averse exploration.

### Multi-step Q-Learning

We make use of  $n$ -step Q-learning (Sutton 1988) to learn both  $Q^{\pi_\omega}$  and  $\tilde{Q}^{\pi_\omega}$ , whereas TempoRL (Biedenkapp et al. 2021) used it only for updating  $\tilde{Q}^{\pi_\omega}$ . We found that  $n$ -step targets can also be used to update  $Q^{\pi_\omega}$ -values without any off-policy correction (Harutyunyan et al. 2016), e.g., importance sampling. Given the sampled  $n$ -step transition  $\tau_t = (s_t, a_t, R_o(s_t, o_{an}), s_{t+n})$  from replay buffer  $\mathcal{R}$ , as long as  $n$  is smaller than or equal to the current extension policy  $\pi_e$ 's output  $j$ , the transition  $\tau_t$  trivially follows our target policy  $\pi_\omega$ . Thus,  $\tau_t$  can be directly used to update the action-value function  $Q^{\pi_\omega}$ . Instead of one step Q-learning in Eq.(1), UTE uses  $n$ -step Q-Learning to update  $Q^{\pi_\omega}$ :

$$\mathcal{L}_{Q^{\pi_\omega}}(\theta) = \mathbb{E}_{\tau_t \sim \mathcal{R}} \left[ \left( Q^{\pi_\omega}(s_t, a_t; \theta) - \sum_{k=0}^{n-1} \gamma^k r_{t+k} - \gamma^n \max_{a'} Q^{\pi_\omega}(s_{t+n}, a'; \bar{\theta}) \right)^2 \middle| n \leq j \sim \pi_e \right]$$

where  $\bar{\theta}$  are the delayed parameters of action-value function  $Q^{\pi_\omega}$  and  $j \sim \pi_e(j_t | s_t, a_t)$ . In general,  $n$ -step returns can be used to propagate rewards faster (Watkins 1989; Peng and Williams 1994). It mitigates the overestimation problem in Q-learning as well (Meng, Gorbet, and Kulić 2021). We empirically illustrate that  $n$ -step learning leads to faster learning in Figure 12b. Note that we don't need to pre-define  $n$  because it is dynamically determined by current extension policy  $\pi_e$ .

### Adaptive Uncertainty Parameter

Instead of fixing the uncertainty parameter  $\lambda$  during the learning process, we propose the adaptive selection of  $\lambda$  utilizing

a non-stationary multi-arm bandit algorithm, as described in (Badia et al. 2020). Consider  $\Lambda$  as the predefined set of uncertainty parameters. At the onset of each episode  $k$ , the bandit selects an arm, denoted by  $\lambda_k \in \Lambda$ , and subsequently receives feedback in the form of episode returns  $R_k(\lambda_k)$ . Given that the reward signal  $R_k(\lambda_k)$  is non-stationary, we employ a sliding-window UCB combined with  $\epsilon_{ucb}$ -greedy exploration to optimize the process. Further details regarding the algorithms can be found in Appendix.

## Experiments

In this section, we present three principal experimental results: Chain MDP, Gridworlds, and Atari 2600 games, as described in Machado et al. (2018) (Machado et al. 2018). Initially, we confirm our hypothesis that a positive  $\lambda$  fosters more aggressive exploration (ChainMDP), while a negative one results in uncertainty-averse exploration (Gridworlds). Subsequently, we demonstrate the significant impact of a well-tuned  $\lambda$  on performance in more complex environments and illustrate that the adaptive selection of  $\lambda$  consistently outperforms other baseline measures (Atari 2600 games). To ensure a fair comparison, we explored a considerable range of hyperparameters to identify the most optimal value for each algorithm (Refer Table 8, 9, 11, and 12 in Appendix)

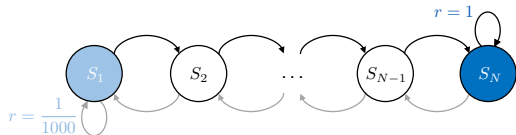


Figure 1: Chain MDP

### Chain MDP

We experimented in the Chain MDP environment as described in Figure 1 (Osband et al. 2016). There are two possible actions {left, right}. If the agent reaches the left end ( $s_1$ ) of the chain and performs a left action, a deceptive small reward (0.001) is given. And if the agent reaches the right end ( $s_n$ ) of the chain and performs a right action, large reward (1.0) is given. Thus, the optimal policy is to take only right actions. Since the reward is very sparse, we need a “deep” exploration strategy to learn the optimal policy. In this toy environment, we will verify our intuition that positive uncertainty parameter  $\lambda$  induces deep exploration and as a result, show a better performance than other baselines, DDQN (Van Hasselt, Guez, and Silver 2016),  $\epsilon z$ -Greedy (Dabney, Ostrovski, and Barreto 2020) and TempoRL (Biedenkapp et al. 2021).

**Setup.** The agent interacts with the environment with a fixed horizon length,  $N + 8$ , where  $N$  is the chain length. Thus, the agent can obtain rewards from zero to 10 in each episode. We limited the maximum extension length as 10 for TempoRL and UTE.

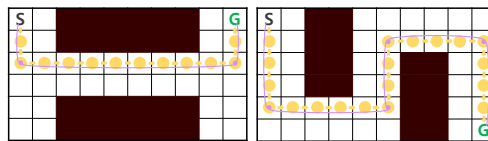
**Exploration-Favor.** Table 1 summarizes the results on various levels of chain length in terms of normalized area under the reward curve (AUC), comparing UTE with the best uncertainty parameter (+2.0, the most optimistic  $\lambda$ ) to  $\epsilon z$ -Greedy

Chain Length	10	30	50	70
$\epsilon z$ -Greedy	0.654	0.427	0.434	0.131
TempoRL	0.904	0.740	0.246	0.052
UTE (ours)	<b>0.919</b>	<b>0.758</b>	<b>0.560</b>	<b>0.191</b>

Table 1: Normalized AUC on Chain MDP over 20 runs

and TempoRL. A reward AUC value closer to 1.0 indicates that the agent was able to find the optimal policy faster. The total training episodes for calculating AUC was set to 1,000 across all chain lengths. The results in the table show that UTE outperforms the other two baselines notably throughout different chain lengths. This implies that UTE has a better exploration strategy which leads to higher reward even in the difficult settings (longer chain length). We also point out that UTE has a smaller variance than TempoRL after it has reached the optimal reward of 10. This is mainly because UTE can collect more diverse samples by exploratory extension policy  $\pi_e$ , which may lead to better generalization and more accurate approximation to the optimal option-value function.

More importantly, we can encode the exploration-favor strategy by adjusting the uncertainty parameter,  $\lambda$ . Note that we don’t use  $\epsilon$ -greedy for the extension policy  $\pi_e$ , whereas TempoRL do. In Appendix, Table 8 shows that more positive  $\lambda$  achieves higher AUC scores. When the agent selects a random action by the  $\epsilon$ -greedy action policy, it can explore deeper by being more optimistic, which leads to faster convergence to the optimal solution. An aggressive exploration strategy is beneficial because the environment has no risky area where the game terminates while repeating the action.



(a) Bridge

(b) ZigZag

Figure 2: 6 × 10 Gridworlds. Agents have to reach a goal state (G) from a starting state (S) detouring the lava. Dots represent decision steps with and without temporally-extended actions.

### Gridworlds

In this section, we analyze the empirical behavior of the various algorithms in the Gridworlds environment *Lava* (Figure 2). It is a 6 × 10 grid with discrete states and actions. An agent starts in the top-left corner and must reach the goal to receive a positive reward (+1) while avoiding stepping into the lava (-1 reward) on its way. In contrast to the chain MDP environment, since we have a risky area “lava”, an uncertainty-averse strategy must be preferred. We compare our method against vanilla DDQN (Van Hasselt, Guez, and Silver 2016)  $\epsilon z$ -Greedy (Dabney, Ostrovski, and Barreto 2020) and TempoRL (Biedenkapp et al. 2021).

**Setup.** We trained all agents for a total of  $3.0 \times 10^3$  episodes using 3 different types of  $\epsilon$ -greedy exploration schedule: linearly decaying from 1.0 to 0.0 over all episodes, logarithmically decaying, and fixed  $\epsilon = 0.1$ . We limited the maximum extension length to be 7. We use neural networks to learn Q-value functions instead of tabular Q-learning.

Env	$\epsilon$ decay	DDQN	TempoRL	$\epsilon_z$ -Greedy	UTE
Bridge	Linear	0.61	0.44	0.76	<b>0.86</b>
	Log	0.54	0.32	0.92	<b>0.92</b>
	Fixed	0.57	0.41	0.59	<b>0.83</b>
Zigzag	Linear	0.38	0.14	0.62	<b>0.84</b>
	Log	0.46	0.12	0.76	<b>0.89</b>
	Fixed	0.34	0.19	0.36	<b>0.76</b>

Table 2: Normalized AUC for reward across different  $\epsilon$  exploration schedules over 20 random seeds.

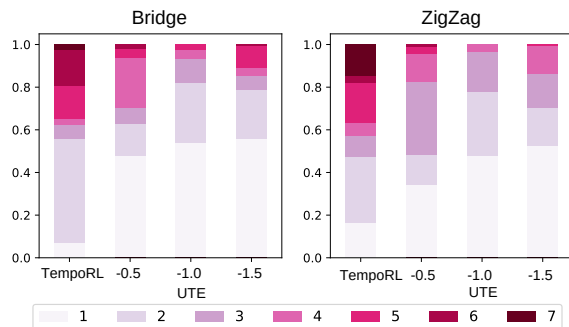


Figure 3: Distributions of extension length in Gridworlds.

**Uncertainty-Averse.** We compare our UTE to the other baselines in terms of normalized area under the reward curve for three different  $\epsilon$ -greedy schedules (see Table 2). Across all  $\epsilon$  exploration strategies, UTE outperforms other methods while showing better performance as uncertainty parameter  $\lambda$  becomes smaller (refer Table 9 in Appendix). This result supports our argument that a pessimistic strategy is preferred in environments with unsafe regions. Furthermore, though exploration rate for  $\pi_a$  is relatively large (e.g. fixed to  $\epsilon = 0.1$ ), UTE consistently shows good performance than others.

Interestingly, the performance of TempoRL is a lot worse than the one described in the original paper (Biedenkapp et al. 2021). It is because we use function approximation to estimate Q-values, rather than tabular Q-learning. Generally, uncontrolled or undesirable overestimation bias can be caused when using function approximation (Moskovitz et al. 2021). Therefore, simply selecting extension length with the highest value leads to a catastrophic result, especially in function approximation setting. Table 2 verifies the fact that pessimistic extension policies perform well in Lava Gridworlds. Moreover, Table 9 in Appendix shows that more negative  $\lambda$  achieves higher AUC scores.

**Coverage.** In Figure 4, we present coverage plots comparing UTE and TempoRL on two types of Lava environments.

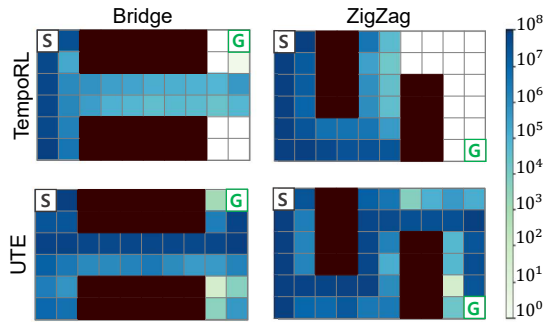


Figure 4: Coverage plots (right) on ZigZag environments. The blue represents states visited more often and white represents states rarely or never seen. See Appendix for the expanded version of the figures.

For UTE, we have set  $\lambda$  to -1.5, a value that has demonstrated robust performance across tests. The results show that UTE provides significantly better coverage over the state space. We can induce our algorithm to repeat sub-optimal action less by using a pessimistic extension policy. Owing to this, our agent can survive for a longer time, leading to better coverage.

**Distribution of Extension Length.** Figure 3 depicts the extension length distributions of TempoRL and UTE on Bridge and ZigZag with logarithmically decaying  $\epsilon$  exploration schedule. More red represents more repetitions. It shows that UTE prefers fewer repetitions compared to TempoRL when  $\lambda < 0$ . As previously articulated in the final paragraph in Preliminaries, observations for long extensions are seldom employed in the process of updating Q-values. Consequently, this propels our algorithm to favor fewer repetitions when  $\lambda < 0$ . In a pessimistic extension policy, the agent tends to refrain from repeating the chosen action many times because the value of a distant state could be much more uncertain than that of a neighbor one.

## Atari 2600: Arcade Learning Environment

In this section, we evaluate the performance of UTE on the Atari benchmark, comparing the following six baseline algorithms: i) vanilla DDQN (Van Hasselt, Guez, and Silver 2016), ii) Fixed Repeat ( $j = 4$ ), iii)  $\epsilon_z$ -Greedy (Dabney, Ostrovski, and Barreto 2020), iv) DAR (Dynamic Action Repetition (Lakshminarayanan, Sharma, and Ravindran 2017)), v) TempoRL (Biedenkapp et al. 2021) vi) B-DQN (Bootstrapped DQN) (Osband et al. 2016). The Fixed Repeat is an algorithm that naively repeats the action a fixed amount of times.

**Setup.** Each algorithm is trained for a total of  $2.5 \times 10^6$  training steps, which is only 10 million frames. All algorithms except B-DQN use a linearly decaying  $\epsilon$ -greedy exploration schedule over the first 200,000 time-steps with a final  $\epsilon$  fixed to 0.01. We evaluated all agents every 10,000 training steps and evaluated for 3 episodes with a very small  $\epsilon$  exploration rate (0.001). We used *OpenAi Gym's* Atari environment with 4 frame-skips (Bellemare et al. 2013). For maximal extension

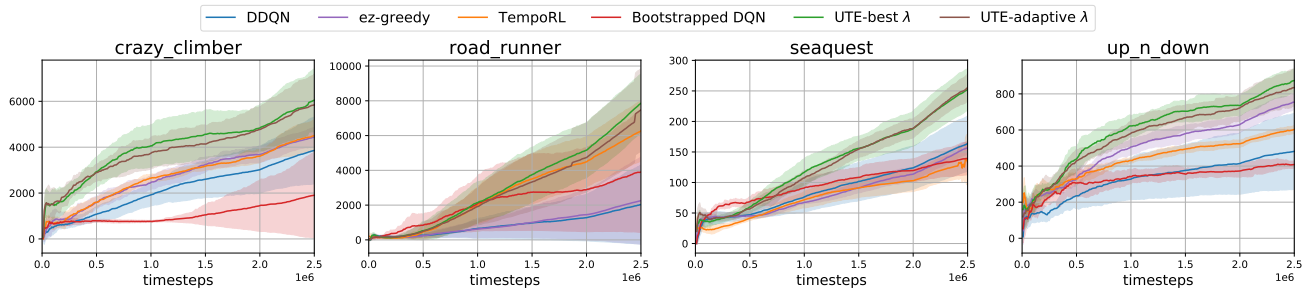


Figure 5: Learning curves of UTE with best  $\lambda$ , UTE with adaptive  $\lambda$  and other baseline algorithms on Atari environments. The shaded area represents the standard deviation over 7 random seeds.

Environment	DDQN	Fixed- $j$	$\epsilon z$ -Greedy	DAR	TempoRL	B-DQN	UTE		
							1-step	$n$ -step	Adaptive $\lambda$
Crazy Climber	5265.8 $\pm 4063.4$	3731.1 $\pm 2997.2$	5295.1 $\pm 3609.7$	2059.1 $\pm 1225.1$	4885.5 $\pm 3378.3$	2961.6 $\pm 3080.0$	6761.9 $\pm 5061.9$	<b>8175.6</b> $\pm 5790.4$	7046.3 $\pm 5350.0$
Road Runner	3277.0 $\pm 4470.3$	1230.3 $\pm 1640.9$	3733.8 $\pm 4716.5$	845.5 $\pm 791.9$	8131.5 $\pm 4099.3$	4976.8 $\pm 6032.6$	4935.6 $\pm 5206.4$	<b>12323.2</b> $\pm 4177.1$	10353.3 $\pm 3283.3$
Sea Quest	207.6 $\pm 124.5$	47.0 $\pm 26.2$	214.5 $\pm 85.6$	42.8 $\pm 33.9$	128.2 $\pm 55.5$	145.1 $\pm 64.5$	206.9 $\pm 92.4$	313.4 $\pm 141.1$	<b>320.3</b> $\pm 159.4$
Up n Down	536.4 $\pm 361.5$	594.8 $\pm 324.6$	823.1 $\pm 320.0$	348.7 $\pm 227.0$	641.5 $\pm 428.6$	383.2 $\pm 242.8$	911.5 $\pm 476.7$	<b>1072.8</b> $\pm 664.0$	990.4 $\pm 707.5$

Table 3: Average rewards and standard deviations (small numbers) over the last 100,000 time steps over Atari environments.

length, we set it to 10.<sup>2</sup>

**Uncertainty-Awareness.** Figure 5 depicts learning curves for UTE and other baseline algorithms (see Figure 13 for full version). And Table 3 summarizes the results of the games in terms of average rewards over the last 100,000 time steps (refer Table 13 for other environments). Overall, UTE achieves higher final rewards than other agents. These results demonstrate that if  $\lambda$  is properly tuned to the environment, our method shows significantly improved performance than existing action repetition methods (DAR,  $\epsilon z$ -Greedy and TempoRL) as well as a deep exploration algorithm (B-DQN). On top of that, we found that the Fixed Repeat algorithm fails at learning in most games. Hence, it is crucial to learn an extension policy for higher performance.

**Effect of  $n$ -step Learning.** We investigate the effect of  $n$ -step Q-learning for the action-value function  $Q^{\pi_\omega}$ , and our empirical results suggest that it helps in most games. Table 3 shows that applying  $n$ -step learning improves performance remarkably. We present the extended version of the ablation study in Figure 12b, which shows a 30.2% improvement (from 1.39 to 1.81) after  $n$ -step Learning has been applied. The result empirically supports our previous argument that off-policy correction is not necessary for our action-repeating options framework.

**Adaptive Uncertainty Parameter  $\lambda$ .** As illustrated in Figure 5 and Table 3, the learning speed of UTE with adaptively chosen  $\lambda$  is somewhat slower compared to the standard UTE. This slight decrease in speed primarily stems from the need for additional samples to optimize  $\lambda$ . Nevertheless, even with

<sup>2</sup>This approach aligns with the settings of Biedenkapp et al. (2021) to ensure a fair comparison.

this adjustment, UTE with an adaptive  $\lambda$  continues to outperform other baseline methods by a considerable margin. These results are particularly encouraging as they obviate the need to predefine the value of  $\lambda$ , thereby reducing the burden of hyperparameter tuning. This aspect of our approach further underscores its practicality and effectiveness in complex learning scenarios.

### Control Problem: Pendulum-v0

In this section, we show that UTE maintains its robustness to continuous control problems where there is a significant chance that repeated actions will surpass the balancing point. Consequently, selecting the appropriate extension length becomes even more crucial. We choose to evaluate on OpenAI gyms (Brockman et al. 2016) Pendulum-v0. Since the action space is continuous, we use DDPG (Lillicrap et al. 2015) as our action policy  $\pi_a$ , thus label it as UTE-DDPG, and apply the adaptive uncertainty parameter technique. The baseline agents are DDPG (Lillicrap et al. 2015), FiGAR (Sharma, Srinivas, and Ravindran 2017), and  $\tau$ -DDPG (TempoRL-DDPG) (Biedenkapp et al. 2021).

**Setup.** We trained all agents for a total of  $3 \times 10^4$  training steps with evaluations conducted every 250 steps. For the initial  $10^3$  steps, a uniform random policy was applied to accumulate initial experiences.

**Robustness to Continuous Control Environment.** In Table 4, UTE-DDPG (with adaptively chosen  $\lambda$ ) demonstrates superior performance, achieving either the top or second-best performance among the benchmarks. This suggests that our algorithm is robust to continuous control environments and consistently outperforms other established action-repeating

algorithms, such as FiGAR and  $\tau$ -DDPG. This advantage can be attributed to our *uncertainty-aware* extension policy that prudently repeats actions. Additionally, UTE exhibits smaller standard deviations than all other baselines, except when the maximal extension length is large (i.e.,  $J = 8$ ), indicating enhanced learning stability.

Max $J$	DDPG	FiGAR	$\tau$ -DDPG	UTE-DDPG
2		-172.7 $\pm 48.6$	-163.2 $\pm 28.6$	<b>-152.6</b> $\pm 17.2$
4	<b>-156.9</b> $\pm 23.2$	$\pm 181.5$ -831.2	$\pm 50.7$ -163.5	<b>-147.4</b> $\pm 17.1$
6		$\pm 427.0$ -1295.0	$\pm 29.0$ -175.3	$\pm 20.8$ <b>-165.0</b>
8		$\pm 274.5$	$\pm 60.3$	$\pm 26.4$

Table 4: Average rewards and standard deviations (small numbers) over the last 10,000 time steps in Pendulum-v0 over various maximal extension lengths ( $J$ ).

## Conclusion

We propose a novel method that learns to repeat actions while explicitly considering the uncertainty over the Q-value estimates of the states reached under the repeated-action option. By calibrating the level of uncertainty considered (denoted by  $\lambda$ ), UTE consistently and significantly outperforms other algorithms, especially those focusing on action repetition, across various environments such as Chain MDP, Gridworlds, Atari 2600, and even in control problems. To our best knowledge, this is the first deep RL algorithm considering uncertainty in the future when instantiating temporally extended actions.

## Acknowledgments

This work was supported by Creative-Pioneering Researchers Program through Seoul National University, and by the National Research Foundation of Korea (NRF) grant funded by the Korea government (MSIT) (No. 2022R1C1C100685912, 2022R1A4A103057912, and RS-2023-00222663).

## References

Anschel, O.; Baram, N.; and Shimkin, N. 2017. Averaged-dqn: Variance reduction and stabilization for deep reinforcement learning. In *International conference on machine learning*, 176–185. PMLR.

Audibert, J.-Y.; Munos, R.; and Szepesvári, C. 2009. Exploration–exploitation tradeoff using variance estimates in multi-armed bandits. *Theoretical Computer Science*, 410(19): 1876–1902.

Auer, P.; Cesa-Bianchi, N.; and Fischer, P. 2002. Finite-time analysis of the multiarmed bandit problem. *Machine learning*, 47: 235–256.

Bacon, P.-L.; Harb, J.; and Precup, D. 2017. The option-critic architecture. In *Proceedings of the AAAI Conference on Artificial Intelligence*, volume 31.

Badia, A. P.; Piot, B.; Kapturowski, S.; Sprechmann, P.; Vitvitskiy, A.; Guo, Z. D.; and Blundell, C. 2020. Agent57: Outperforming the atari human benchmark. In *International Conference on Machine Learning*, 507–517. PMLR.

Bai, C.; Wang, L.; Han, L.; Hao, J.; Garg, A.; Liu, P.; and Wang, Z. 2021. Principled exploration via optimistic bootstrapping and backward induction. In *International Conference on Machine Learning (ICML 2021)*, 577–587. PMLR.

Barreto, A.; Borsa, D.; Hou, S.; Comanici, G.; Aygün, E.; Hamel, P.; Toyama, D.; Mourad, S.; Silver, D.; Precup, D.; et al. 2019. The option keyboard: Combining skills in reinforcement learning. *Advances in Neural Information Processing Systems*, 32.

Bellemare, M.; Srinivasan, S.; Ostrovski, G.; Schaul, T.; Sutton, D.; and Munos, R. 2016. Unifying count-based exploration and intrinsic motivation. *Advances in neural information processing systems*, 29.

Bellemare, M. G.; Naddaf, Y.; Veness, J.; and Bowling, M. 2013. The arcade learning environment: An evaluation platform for general agents. *Journal of Artificial Intelligence Research*, 47: 253–279.

Biedenkapp, A.; Rajan, R.; Hutter, F.; and Lindauer, M. 2021. TempoRL: Learning When to Act. In *Proceedings of the 38th International Conference on Machine Learning (ICML 2021)*.

Brockman, G.; Cheung, V.; Pettersson, L.; Schneider, J.; Schulman, J.; Tang, J.; and Zaremba, W. 2016. Openai gym. *arXiv preprint arXiv:1606.01540*.

Chen, R. Y.; Schulman, J.; Abbeel, P.; and Sidor, S. 2017. UCB and infogain exploration via q-ensembles. *arXiv preprint arXiv:1706.01502*, 9.

Da Silva, F. L.; Hernandez-Leal, P.; Kartal, B.; and Taylor, M. E. 2020. Uncertainty-aware action advising for deep reinforcement learning agents. In *Proceedings of the AAAI conference on artificial intelligence*, volume 34, 5792–5799.

Dabney, W.; Ostrovski, G.; and Barreto, A. 2020. Temporally-Extended  $\epsilon$ -Greedy Exploration. In *9th International Conference on Learning Representations, ICLR 2021*.

Dayan, P.; and Hinton, G. E. 1992. Feudal reinforcement learning. *Advances in neural information processing systems*, 5.

Efron, B. 1982. *The jackknife, the bootstrap and other resampling plans*. SIAM.

Fikes, R. E.; Hart, P. E.; and Nilsson, N. J. 1972. Learning and executing generalized robot plans. *Artificial intelligence*, 3: 251–288.

Garivier, A.; and Moulines, E. 2008. On upper-confidence bound policies for non-stationary bandit problems. *arXiv preprint arXiv:0805.3415*.

Harutyunyan, A.; Bellemare, M. G.; Stepleton, T.; and Munos, R. 2016. Q ( $\lambda$ ) with Off-Policy Corrections. In *International Conference on Algorithmic Learning Theory*, 305–320. Springer.

Lakshminarayanan, A.; Sharma, S.; and Ravindran, B. 2017. Dynamic action repetition for deep reinforcement learning. In

- Proceedings of the AAAI Conference on Artificial Intelligence*, volume 31.
- Lee, S.; Seo, Y.; Lee, K.; Abbeel, P.; and Shin, J. 2022. Offline-to-online reinforcement learning via balanced replay and pessimistic q-ensemble. In *Conference on Robot Learning*, 1702–1712. PMLR.
- Lillicrap, T. P.; Hunt, J. J.; Pritzel, A.; Heess, N.; Erez, T.; Tassa, Y.; Silver, D.; and Wierstra, D. 2015. Continuous control with deep reinforcement learning. *arXiv preprint arXiv:1509.02971*.
- Machado, M. C.; Barreto, A.; and Precup, D. 2021. Temporal Abstraction in Reinforcement Learning with the Successor Representation. *arXiv preprint arXiv:2110.05740*.
- Machado, M. C.; Bellemare, M. G.; Talvitie, E.; Veness, J.; Hausknecht, M. J.; and Bowling, M. 2018. Revisiting the Arcade Learning Environment: Evaluation Protocols and Open Problems for General Agents. *Journal of Artificial Intelligence Research*, 61: 523–562.
- Meng, L.; Gorbet, R.; and Kulić, D. 2021. The effect of multi-step methods on overestimation in deep reinforcement learning. In *2020 25th International Conference on Pattern Recognition (ICPR)*, 347–353. IEEE.
- Metelli, A. M.; Mazzolini, F.; Bisi, L.; Sabbioni, L.; and Restelli, M. 2020. Control frequency adaptation via action persistence in batch reinforcement learning. In *International Conference on Machine Learning (ICML 2020)*, 6862–6873. PMLR.
- Mnih, V.; Kavukcuoglu, K.; Silver, D.; Rusu, A. A.; Veness, J.; Bellemare, M. G.; Graves, A.; Riedmiller, M.; Fidjeland, A. K.; Ostrovski, G.; et al. 2015. Human-level control through deep reinforcement learning. *Nature*, 518(7540): 529–533.
- Moskovitz, T.; Parker-Holder, J.; Pacchiano, A.; Arbel, M.; and Jordan, M. 2021. Tactical optimism and pessimism for deep reinforcement learning. *Advances in Neural Information Processing Systems*, 34.
- Osband, I.; Blundell, C.; Pritzel, A.; and Van Roy, B. 2016. Deep exploration via bootstrapped DQN. In *Advances In Neural Information Processing Systems 29*, 4026–4034.
- Park, S.; Kim, J.; and Kim, G. 2021. Time Discretization-Invariant Safe Action Repetition for Policy Gradient Methods. *Advances in Neural Information Processing Systems*, 34.
- Parr, R.; and Russell, S. 1997. Reinforcement learning with hierarchies of machines. *Advances in neural information processing systems*, 10.
- Peer, O.; Tessler, C.; Merlis, N.; and Meir, R. 2021. Ensemble bootstrapping for Q-Learning. In *International Conference on Machine Learning*, 8454–8463. PMLR.
- Peng, J.; and Williams, R. J. 1994. Incremental multi-step Q-learning. In *Machine Learning Proceedings 1994*, 226–232. Elsevier.
- Precup, D. 2000. *Temporal abstraction in reinforcement learning*. University of Massachusetts Amherst.
- Puterman, M. L. 2014. *Markov decision processes: discrete stochastic dynamic programming*. John Wiley & Sons.
- Schoknecht, R.; and Riedmiller, M. 2002. Speeding-up reinforcement learning with multi-step actions. In *International Conference on Artificial Neural Networks*, 813–818. Springer.
- Sharma, S.; Srinivas, A.; and Ravindran, B. 2017. Learning to repeat: Fine grained action repetition for deep reinforcement learning. In *5th International Conference on Learning Representations, ICLR 2017*.
- Stolle, M.; and Precup, D. 2002. Learning options in reinforcement learning. In *International Symposium on abstraction, reformulation, and approximation*, 212–223. Springer.
- Sutton, R. S. 1988. Learning to predict by the methods of temporal differences. *Machine learning*, 3(1): 9–44.
- Sutton, R. S.; Precup, D.; and Singh, S. 1999. Between MDPs and semi-MDPs: A framework for temporal abstraction in reinforcement learning. *Artificial intelligence*, 112(1-2): 181–211.
- Thrun, S.; and Schwartz, A. 1993. Issues in using function approximation for reinforcement learning. In *Proceedings of the 1993 Connectionist Models Summer School Hillsdale, NJ. Lawrence Erlbaum*, volume 6.
- Touati, A.; Satija, H.; Romoff, J.; Pineau, J.; and Vincent, P. 2020. Randomized value functions via multiplicative normalizing flows. In *Uncertainty in Artificial Intelligence*, 422–432. PMLR.
- Van Hasselt, H.; Guez, A.; and Silver, D. 2016. Deep reinforcement learning with double q-learning. In *Proceedings of the AAAI conference on artificial intelligence*, volume 30.
- Watkins, C. J.; and Dayan, P. 1992. Q-learning. *Machine learning*, 8(3): 279–292.
- Watkins, C. J. C. H. 1989. Learning from delayed rewards.
- Xia, L.; and Collins, A. G. 2021. Temporal and state abstractions for efficient learning, transfer, and composition in humans. *Psychological review*.
- Zahavy, T.; Haroush, M.; Merlis, N.; Mankowitz, D. J.; and Mannor, S. 2018. Learn what not to learn: Action elimination with deep reinforcement learning. *Advances in Neural Information Processing Systems*, 31.

## Details of Baselines

**Fixed Repeat.** Fixed Repeat in Atari experiment corresponds to a DDQN agent that always repeats the action for a fixed amount of times. In other words, the extension policy returns the same  $j$  at every decision time. In our settings,  $j$  is set to 4 (see Figure 11 for performance of other  $j$ s). The reason for evaluating this naive method is to confirm that this approach fails, highlighting the importance of the extension length.

**Temporally-Extended  $\epsilon$ -Greedy.**  $\epsilon z$ -Greedy (Dabney, Ostrovski, and Barreto 2020) is a simple add-on to the  $\epsilon$ -greedy policy. The agent follows the current policy for one step with probability  $1 - \epsilon$ , or with probability  $\epsilon$  samples an action  $a$  from a uniform random distribution and repeats it for  $j$  times, which is drawn from a pre-defined duration distribution. We used the heavy-tailed zeta distribution, with  $\mu = 1.25$  as the duration distribution in the Chain MDP and the Gridworlds environment. This was done by conducting a hyperparameter search on  $\mu$  for the set  $\{1.25, 1.5, 2.0, 2.5, 3.0\}$ . In Atari games, we choose the best per-game  $\mu$  among the set  $\{1.5, 1.75, 2.0, 2.25, 2.5\}$  for a fair comparison to our UTE. A combination of  $\epsilon$  chance to explore and zeta-distributed duration is called  $\epsilon z$ -greedy exploration.

The experimental results from (Dabney, Ostrovski, and Barreto 2020) show that  $\epsilon z$ -Greedy incorporated in existing R2D2 and Rainbow agents result higher median human-normalized score over the 57 Atari games. However, this algorithm is highly dependent on the exploration rate  $\epsilon$ , which can cause difficulties in online learning.

**Dynamic Action Repetition.** DAR (Lakshminarayanan, Sharma, and Ravindran 2017) is a framework for discrete-action space deep RL algorithms. DAR duplicates the output heads twice such that an agent can choose from  $2 \times |\mathcal{A}|$  actions. And each output heads corresponds to pre-defined repetition values,  $r_1, r_2$ , where  $r_1$  and  $r_2$  are fixed hyper parameters. Hence, action  $a_k$  is repeated  $r_1$  number of times if  $k < |\mathcal{A}|$  and  $r_2$  number of times if  $k \geq |\mathcal{A}|$ . In our experiments,  $r_1$  is fixed to maximum extension length  $J$  and  $r_2$  to 1 to allow for actions at every time step.

There are some drawbacks to this approach. First,  $r_1$  and  $r_2$  have to be predefined, which means we need prior knowledge of the environments. And also, the learning process becomes a lot more difficult because the action space doubled.

**TempoRL.** TempoRL (Biedenkapp et al. 2021) proposes a “flat” hierarchical structure in which *behavior* policy ( $\pi_a$ ) determines the action  $a$  to be played given the current state  $s$ , and a *skip* policy ( $\pi_j$ ) determines how long to repeat this action. The flat hierarchical structure refers to *behavior* policy and *skip* policy having to make decisions at the same time-step. The action policy has to be always queried before the skip policy. When an agent plays a chosen action for extension length  $j$ , total of  $\frac{j(j+1)}{2}$  skip-transitions are observed and stored in the replay buffer. The *behavior* and the *skip* Q-functions can be updated using one-step observations and the overarching skip-observation. Using the samples collected, the *behavior* policy can be learned by a classical one step Q-learning. The  $n$ -step Q-learning is used to learn the *skip* value with the condition that, at each step in the  $j$  steps, the action stays the same.

**Bootstrapped DQN.** B-DQN (Osband et al. 2016) is an algorithm for temporally-extended (or deep) exploration. Inspired by Thompson sampling, it selects an action without the need for an intractable exact posterior update. Osband et al. (2016) suggest bootstrapped neural nets can produce reasonable posterior estimates. The network of bootstrapped DQN consists of a shared architecture with  $K$  bootstrapped “heads” stretching off independently. Each head is initialized randomly and trained only on its bootstrapped sub-sample of the data. The shared network learns a joint feature representation across all the data. For evaluation, an ensemble voting policy is used to decide action.

**FiGAR.** FiGAR (Sharma, Srinivas, and Ravindran 2017) is a framework tailored for both discrete and continuous action spaces. Unlike the DAR method where a single policy learns both the action selection and its duration, FiGAR separates these tasks using two distinct policies:  $\pi_a : \mathcal{S} \rightarrow \mathcal{A}$  for action selection and  $\pi_r : \mathcal{S} \rightarrow \{1, 2, \dots, \text{max repetition}\}$  for determining repetition duration. During the training process, given a state  $s$ ,  $\pi_a$  chooses the action while  $\pi_r$  simultaneously determines how long that action should be repeated starting from  $s$ . Crucially, when making their selections, neither  $\pi_a$  nor  $\pi_r$  has knowledge of the other’s decision. This ensures that the action and its repetition duration are chosen independently.

## Implementation Details: UTE

### Bootstrap with random initialization for option-value functions

Formally, we consider an ensemble of  $B$  option-value functions,  $\{\tilde{Q}_{(b)}^{\pi_\omega}\}_{b=1}^B$ , where  $\pi_\omega$  denotes the policy over option. To train the ensemble of option-value functions  $\tilde{Q}_{(b)}^{\pi_\omega}$ , we use two mechanisms to enforce diversity between these Q-functions (Efron 1982; Osband et al. 2016): The first mechanism is random-initialization of model parameters for each option-value functions to induce initial diversity in the models. The second mechanism is to train each Q-function with different samples. Specifically, in each timestep  $t$ , each  $b^{\text{th}}$  Q-function is trained by multiplying binary mask  $m_{t,b}$  to each objective function, where the binary mask  $m_{t,b}$  is sampled from the Bernoulli distribution ( $p$ ) with parameter  $\beta \in (0, 1]$ . In our experiments, we use  $p = 0.5$  for the parameter of the Bernoulli distribution.

### Multi-step target for both action- and option-value functions

We learn parameterized estimates of Q-value functions, an action-value function  $Q^{\pi_\omega}(s, a; \theta) \approx Q^{\pi_\omega^*}(s, a)$  and an option-value function  $\tilde{Q}^{\pi_\omega}(s, \omega_{aj}; \phi) \approx \tilde{Q}^{\pi_\omega^*}(s, \omega_{aj})$ , using neural networks. We use two different neural network function approximators

parameterized by  $\theta$  and  $\phi$  respectively. For stability, we integrate double Q-learning (Van Hasselt, Guez, and Silver 2016) technique. We use multi-step Q-learning to update both action-value function  $Q^{\pi_\omega}$  and option-value function  $\tilde{Q}^{\pi_\omega}$ . The following equations represent Bellman residual errors of action- and option-value functions respectively:

$$\mathcal{L}_{Q^{\pi_\omega}}(\theta) = \mathbb{E}_{\tau_t \sim \mathcal{R}} \left[ (Q^{\pi_\omega}(s_t, a_t; \theta) - \sum_{k=0}^{n-1} \gamma^k r_t - \gamma^n \max_{a'} Q^{\pi_\omega^*}(s_{t+n}, a'; \bar{\theta}))^2 \mid n \leq j \sim \pi_e \right] \quad (5)$$

$$\mathcal{L}_{\tilde{Q}^{\pi_\omega}}(\phi) = \mathbb{E}_{\tau_t \sim \mathcal{R}} \left[ \sum_{b=1}^B \left[ m_{t,b} (\tilde{Q}_b^{\pi_\omega}(s_t, \omega_{aj}; \phi) - \sum_{k=0}^{j-1} \gamma^k r_t - \gamma^j \max_{a'} Q^{\pi_\omega^*}(s_{t+j}, a'; \bar{\theta}))^2 \right] \right] \quad (6)$$

where  $\tau_t$  is a multi-step transition trajectory sampled from a replay buffer  $\mathcal{R}$ ,  $m_{t,b}$  is a binary bootstrap mask, and  $\bar{\theta}$  are the delayed parameters of action-value function  $Q^{\pi_\omega}$ . The delayed parameters are the parameters of the target network for action-value function  $Q^{\pi_\omega}$ . The target network with the delayed parameters is the same as the online network except that its parameters are copied every  $\tau$  step from the online network, and kept fixed on all other steps (Mnih et al. 2015). Note that  $n$  for  $n$ -step learning in Eq.(5) has to follow the current extension policy  $\pi_e$ . Therefore, in order to update action-value function  $Q^{\pi_\omega}$  in Eq.(5), we only use trajectory samples in which the extension length is smaller than or equal to the output of current extension policy, i.e.  $n \leq j \sim \pi_e(j_t \mid s_t, a_t)$ .

One interesting point of the above equations is that we use the same target value for both Q-functions:  $Q^{\pi_\omega}$  in Eq.(5) and  $\tilde{Q}^{\pi_\omega}$  Eq.(6). Trivially, we can demonstrate that the target value for the option selection of repeated actions is the same as one for single-step action selection within the option, i.e.  $\max_{a'} Q^{\pi_\omega^*}(s_{t+j}, a') = \max_{\omega'} Q^{\pi_\omega^*}(s_{t+j}, \omega'_{aj})$ . By using the same target value, we can stabilize the learning process.

### The Same Target for both action- and option- value functions

On the fourth page of the main paper, we argue that we can use the same target for both types of Q-values. The following proposition formalizes the statement. Though it is a trivial result, we simply present the proof of it for better comprehension.

*Proof of Proposition 1.* For any  $s \in \mathcal{S}$ , define the value of executing an action in the context of a state-option pair as  $Q_U : \mathcal{S} \times \Omega \times \mathcal{A} \rightarrow \mathbb{R}$ . Let  $\pi_U(a \mid s, \omega_{aj}) : \mathcal{S} \times \Omega \rightarrow \mathcal{P}(\mathcal{A})$  be an *intra-option* policy (Sutton, Precup, and Singh 1999), which returns an action  $a$  when executing an option  $\omega_{aj}$  at state  $s$ . Then, option-value functions can be written as:

$$\begin{aligned} \tilde{Q}^{\pi_\omega}(s, \omega_{aj}) &= \sum_{a'} \pi_U(a' \mid s, \omega_{aj}) Q_U(s, \omega_{aj}, a') = \sum_{a'} \mathbf{1}_a Q_U(s, \omega_{aj}, a') \\ &= Q_U(s, \omega_{aj}, a), \end{aligned} \quad (7)$$

where the second equality holds since  $\pi_U$  deterministically returns action  $a$ . Therefore we have,

$$\begin{aligned} V^{\pi_\omega^*}(s_0) &= \max_{\omega_{aj}} \tilde{Q}^{\pi_\omega^*}(s_0, \omega_{aj}) = \max_{a,j} \tilde{Q}^{\pi_\omega^*}(s_0, \omega_{aj}) = \max_{a,j} Q_U^*(s, \omega_{aj}, a) \\ &= \max_a \left\{ \max_j Q_U^*(s, \omega_{aj}, a) \right\} = \max_a Q^{\pi_\omega^*}(s, a), \end{aligned}$$

where the second equality holds since  $\omega_{aj}$  is determined by an action  $a$  and extension length  $j$ , the third equality is by Eq.(7), and the last equality holds since  $\pi_\omega^*$  is the optimal policy. This concludes the proof.  $\square$

## Experiments Details

All experiments were run on an internal cluster containing GeForce RTX 3090 GPUs. Atari experiments took 13 hours to train for 10 million frames on GPU. Our Chain MDP environment and B-DQN baseline implementation is based on code from Touati et al. (2020). The license for this asset is Attribution-NonCommercial 4.0 International. Gridworlds and Atari environment settings along with TempoRL baseline implementation is from Biedenkapp et al. (2021). This asset is licensed under Apache License 2.0. The Arcade Learning Environment (ALE) (Bellemare et al. 2013) for Atari games is licensed under the GNU General Public License Version 2.

### Chain MDP experiment

**Network Architecture.** In the Chain MDP experiment, all agents, i.e.  $\epsilon z$ -Greedy, TempoRL, and UTE, use simple DQN architecture (Mnih et al. 2015) for their action policy. The network consists of 3 dense layers with a ReLU activation function. The number of hidden nodes is set to 16 for all dense layers.

TempoRL has another output stream that combines a hidden layer with 10 units together with the output of the second fully connected layer. It is followed by a fully connected layer that outputs predicted Q-values, extension lengths.

In order to implement extension policy  $\pi_e$  of UTE, the agent has another ensemble network of 10 identical neural networks. Each of these 10 ensemble networks is a 3-layer neural network with fully connected layers with 26 hidden units, where the input is a concatenation of the state and the chosen action.

Hyper-parameter	Value
Discount rate	0.999
Target update frequency	500
Initial $\epsilon$	1.0
Final $\epsilon$	0.001
$\epsilon$ time-steps	$N \times 100$
Loss Function	Huber Loss
Optimizer	Adam
Learning rate	0.0005
Batch Size	64
Replay buffer size	$5 \times 10^4$
Extension replay buffer size	$5 \times 10^4$
Number of ensemble heads	10
Max extension length ( $J$ )	10, 15, 20
Uncertainty parameter ( $\lambda$ )	-2, -1, 0, 1, 2

Table 5: Hyper-parameters used for the Chain MDP experiments

### Gridworlds experiment

**Network Architecture.** In the Gridworlds experiment, all agents, i.e. DDQN, TempoRL and UTE, were trained using deep Q-network (Mnih et al. 2015) with 3 dense layers. The number of each hidden node is 50 and ReLU activation function was used for non-linearity. All of the agents were implemented using double DQN (Van Hasselt, Guez, and Silver 2016). Both TempoRL and UTE agents have separate network for extension policy.

For extension policy, TempoRL uses a single 3-layer neural network with fully connected layers of 50, 50, and 50 units, whereas our UTE uses 10 duplicated networks of a 3-layer neural network with fully connected layers of 50, 50, and 50 units. The input of extension policy is a concatenation of the state and the chosen action, which is the same as the Chain MDP experiment.

Hyper-parameter	Value
Discount rate	0.99
Initial $\epsilon$	1.0
Final $\epsilon$	0.0
$\epsilon$ time-steps	50
Loss Function	MSE Loss
Optimizer	Adam
Learning rate	0.001
Batch Size	64
Replay buffer size	$10^6$
Extension replay buffer size	$10^6$
Number of ensemble heads	10
Max extension length ( $J$ )	7
Uncertainty parameter ( $\lambda$ )	-1.5, -1.0, -0.5

Table 6: Hyper-parameters used for the Gridworlds experiments

### Atari experiment

**Network Architecture.** The input size of images is  $84 \times 84$ , and the last 4 frames of this image are stacked together. This will be our input throughout the experiment.

**DDQN** agent uses the same architecture for DQN of (Mnih et al. 2015) with the target network (Van Hasselt, Guez, and Silver 2016). This architecture has 3 convolutional layers of 32, 64 and 64 feature planes with kernel sizes of 8,4 and 3, and strides of 4,2, and 1, respectively. These are followed by a fully connected network with 512 hidden units followed by another fully connected layer to the Q-Values for each action.

$\epsilon$ -**Greedy** agent uses the exact same architecture as Mnih et al. (2015). The only difference with DDQN is that  $\epsilon$ -Greedy repeats an exploratory action, which is sampled from uniform random distribution. And the extension length  $j$  is sampled from zeta distribution. The hyper-parameter  $\mu$  for zeta distribution is set depending on the experiments: 1.25 for Chain-MDP and Gridworlds, and the best one for each game in Atari experiment.

Hyper-parameter	Value
Discount rate	0.99
Gradient Clip	40.0
Target update frequency	500
Learning starts	10 000
Initial $\epsilon$	1.0
Final $\epsilon$	0.01
Evaluation $\epsilon$	0.001
$\epsilon$ time-steps	200 000
Train frequency	4
Loss Function	Huber Loss
Optimizer	Adam
Learning rate	0.0001
Batch Size	32
Extension Batch Size	32
Replay buffer size	$5 \times 10^4$
Extension replay buffer size	$5 \times 10^4$
Number of ensemble heads	10
Max extension length ( $J$ )	10
Uncertainty parameter ( $\lambda$ )	-1.5, -1.0, -0.5, -0.2, 0.0, 0.2, 0.5, 1.0

Table 7: Hyper-parameters used for the Atari experiments

**DAR** agent selects action and extension length based on  $2 \times |\mathcal{A}|$  Q-values. Therefore, the output of the last layer is duplicated and the duplicate outputs corresponding to a different extension length,  $r_1$  and  $r_2$ . The hyper-parameters,  $r_1$  and  $r_2$ , are set to 1 and 10 respectively.

**TempoRL** agent uses the shared architecture, the structure of which is the same as one described in Biedenkapp et al. (2021). On top of DQN architecture (Mnih et al. 2015), an additional output stream for the extension length is incorporated. The extension length is embedded into a 10-dimensional vector and then concatenated with the output of the last convolutional layer of the network. The features then pass through two fully connected hidden layers, each with 512 units.

**B-DQN** has one torso network of 3 convolutional layers, which is the same as that of DQN (Mnih et al. 2015). However, it has 10 heads branching off independently (Osband et al. 2016). Each head consists of two fully connected hidden layers, each with 512 units. Therefore the agent returns 10 Q-values from each head.

**UTE** uses the similar architecture as that of TempoRL (Biedenkapp et al. 2021). The main difference compared to TempoRL is that UTE uses an ensemble method for the output stream of extension length. After concatenating a 10-dimensional extension length vector and the output of the last convolutional layer, the concatenated vector pass through 10 heads branching off independently. Each 10 head consists of fully connected layer with 512 hidden units followed by a fully connected layer to the Q-Values for each extension length.

## Further Experimental Results

### Chain MDP

**Uncertainty Parameter.** Table 8 shows the effect of the uncertainty parameter on normalized AUC score for 1,000 training episodes. We can see that an exploration-favoring high uncertainty parameter is beneficial in the Chain MDP environment. The longer the chain length, the more sensitive it becomes sensitive to the uncertainty parameter. In the chain length of 70, UTE with uncertainty parameter +2 is a lot better than the one with uncertainty parameter -2. This result indicates that optimistically repeating the chosen action could lead to good performance if there is no risky area in the environment. The Table also shows that for  $\epsilon z$ -Greedy with  $\mu = 1.25$  performed the best, and we used the value for the experiments.

**Maximum Repeat  $J$ .** We can also predispose the agent to repeat actions in larger numbers by increasing another parameter, the maximum extension length  $J$ . However, increasing the maximum extension length is not always a good solution as it increases the size of the set of extension lengths,  $|\mathcal{J}|$ , slowing down the learning process. As exhibited in Figure 6, the small maximum extension length is detrimental to the agent’s performance. Note that the degree of exploration of  $\epsilon z$ -Greedy is affected by the hyperparameter  $\mu$  for zeta distribution, and the value is fixed to 1.25 throughout the chain MDP experiments. While TempoRL is sensitive to extension length especially when the chain length is long, our UTE is quite robust to changes in extension length. We can see that UTE agent reaches the highest final performance compared to other agents.

Chain Length	TempoRL	$\epsilon z$ -Greedy ( $\mu$ )					UTE ( $\lambda$ )				
		1.25	1.5	2.0	2.5	3.0	-2.0	-1.0	0.0	1.0	2.0
10	0.90	<b>0.65</b>	0.61	0.48	0.46	0.46	0.88	0.91	0.90	0.92	<b>0.92</b>
30	0.74	<b>0.43</b>	0.42	0.42	0.38	0.27	0.45	0.55	0.62	0.73	<b>0.76</b>
50	0.25	<b>0.43</b>	0.40	0.23	0.17	0.05	0.07	0.05	0.37	0.47	<b>0.67</b>
70	0.05	<b>0.13</b>	0.12	0.03	0.04	0.1	0.01	0.01	0.01	0.07	<b>0.19</b>

Table 8: Normalized AUC for rewar across different agents over 20 random seeds. Maximum extension length for TempoRL and UTE is set to 10. The numbers in the brackets of UTE represent the uncertainty parameter,  $\lambda$ . We can see that greater uncertainty parameters show better performance, especially in the difficult settings where the chain length is long.

## Gridworlds

In the following additional results, we supplement one more environment called Cliff in addition to Bridge and Zigzag. Same as others, the Cliff is discrete, deterministic, and has a  $6 \times 10$  size with sparse rewards. Note that all agents are implemented by function approximation, not tabular setting.

**Uncertainty Parameter** Table 9 shows an uncertainty-averse (negative uncertainty parameter) is beneficial in the Gridworlds environment where there are risky area (Lava). Combined with the result of Figure 8, we empirically verified that more negative  $\lambda$  induce more pessimistic behavior, which can lead to better performance. The Table also shows that for  $\epsilon z$ -Greedy with  $\mu = 1.25$  performed good in overall, and we used the value for the experiments.

**Learning curve.** In Figure 9, we plot all the learning curves of three agents across three different Lava environments and three different exploration schedules. In this result, we observe that UTE converges to the optimal solution faster than other baselines, showing low standard deviations. Also, our UTE is robust to varying exploration strategies even using sub-optimal ones such as Fixed  $\epsilon$ . One more interesting point is that TempoRL performs worse than vanilla DDQN. These results contradict the ones of Biedenkapp et al. (2021), which experimented in a tabular setting instead of function approximation. Generally, when using function approximation to estimate Q-values, it is more likely to choose sub-optimal action  $a$ . Therefore, in this case, it is necessary to consider uncertainty in estimated values for safely repeating the chosen action. By inducing pessimism ( $\lambda < 0$ ) to the extension policy  $\pi_e$ , the agent can repeat the chosen sub-optimal action  $a$  less, which leads to a safer learning.

**Coverage.** Figure 7 illustrates state visitation coverage of different agents for 3 different gridworlds environments. Both TempoRL and UTE repeat the chosen actions, which can lead to a better exploration. However, TempoRL is not any better than vanilla DDQN, whereas our UTE shows significantly better coverage. This implies that a pessimistic extension policy inducing safe exploration can result in better coverage of the state space.

**Distribution of extension length.** The full version of distributions of extension length is presented in Figure 8. It shows that the TempoRL selects large extension length, close to 7, more often than our UTE. We can see UTE maneuver at a smaller scale as the uncertainty parameter decreases to induce more pessimistic behavior. The portion of small extension lengths tends to increase as being more pessimistic.

Environment		$\epsilon z$ -Greedy ( $\mu$ )					UTE ( $\lambda$ )		
		1.25	1.5	2.0	2.5	3.0	-0.5	-1.0	-1.5
Cliff	Linear	<b>0.80</b>	0.79	0.79	0.78	0.77	0.89	0.88	<b>0.90</b>
	Log	0.92	<b>0.93</b>	0.91	0.84	0.81	0.94	0.95	<b>0.96</b>
	Fixed	<b>0.65</b>	0.64	0.64	0.64	0.63	0.84	0.84	<b>0.85</b>
Bridge	Linear	0.75	0.75	<b>0.76</b>	0.74	0.73	0.83	0.84	<b>0.86</b>
	Log	<b>0.92</b>	0.92	0.91	0.90	0.89	0.85	0.88	<b>0.92</b>
	Fixed	<b>0.59</b>	0.57	0.58	0.55	0.55	0.72	0.82	<b>0.83</b>
Zigzag	Linear	0.62	<b>0.63</b>	0.61	0.61	0.62	0.73	0.82	<b>0.84</b>
	Log	<b>0.76</b>	0.72	0.63	0.61	0.52	0.66	0.86	<b>0.89</b>
	Fixed	0.36	0.40	0.41	0.42	<b>0.43</b>	0.62	0.70	<b>0.76</b>

Table 9: Normalized AUC of reward for varying hyperparameters of  $\mu$  in  $\epsilon z$ -Greedy and  $\lambda$  in UTE on a logarithmically decaying  $\epsilon$ -strategy in the Gridworlds environment. (20 random seeds)

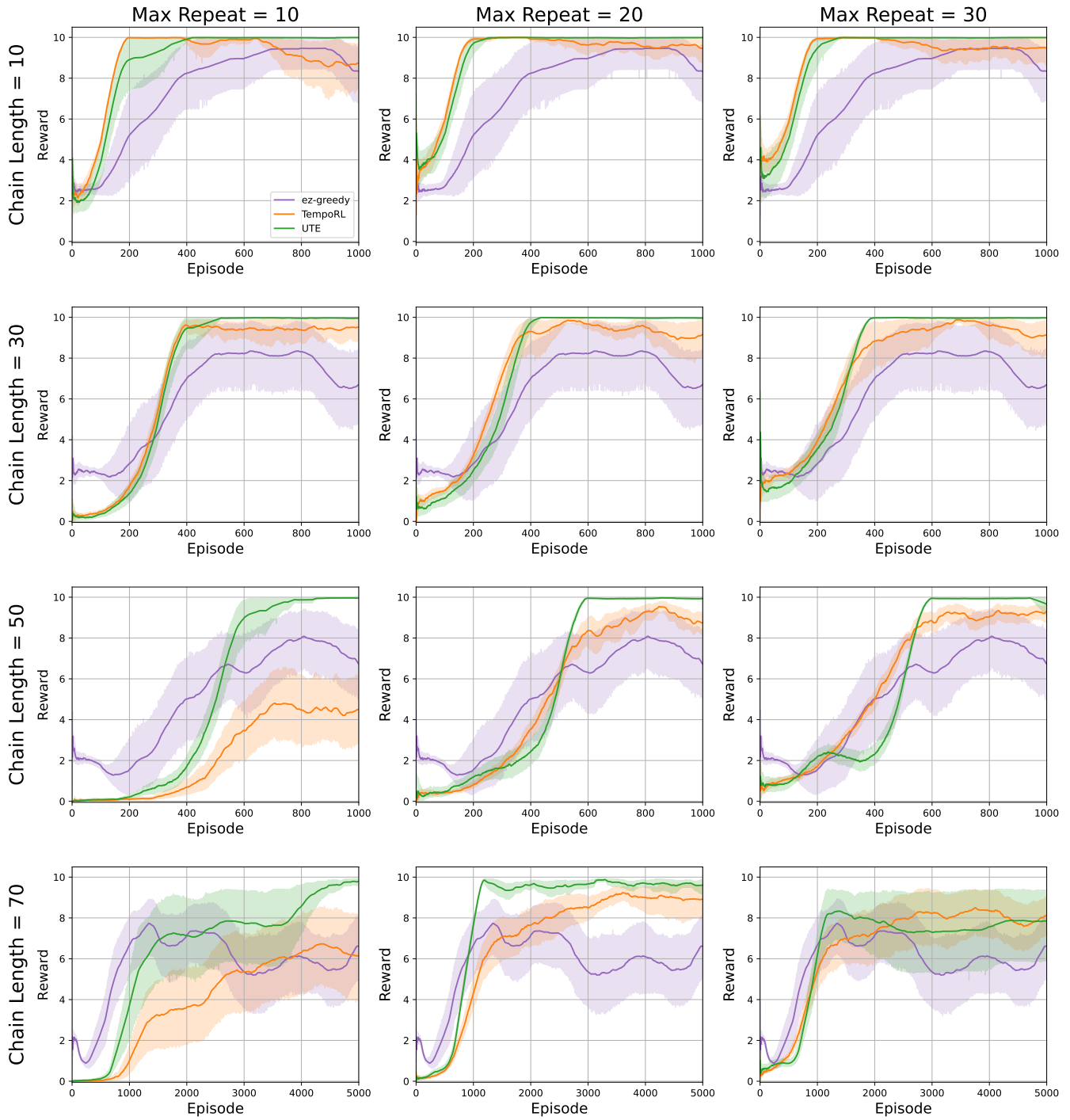


Figure 6: Training reward for  $\epsilon$ -Greedy, TempoRL, and UTE in the Chain MDP environment. The horizontal axis represents the maximum extension length of 10, 20, and 30 from left to right, respectively. The vertical axis represents the chain length of 10, 30, 50, and 70 from top to bottom. Learning curve for  $N = 70$  is presented with 5,000 training episodes. (20 random seeds)

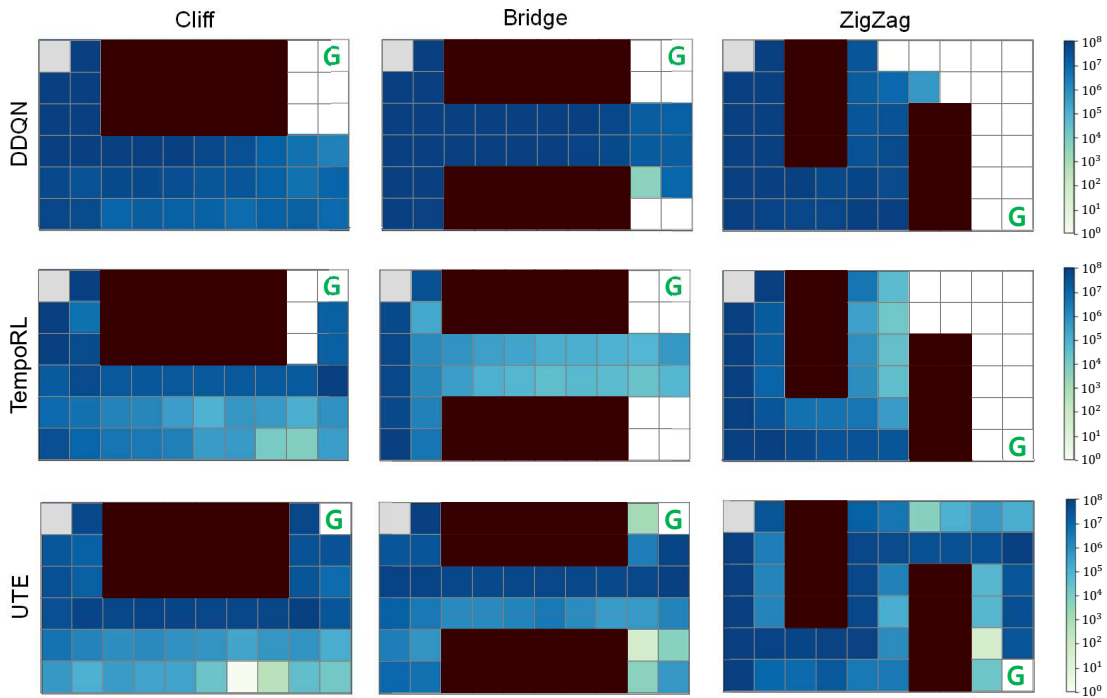


Figure 7: Coverage plots on all Lava environments, comparing UTE ( $\lambda=-1.5$ ) to DDQN and TempoRL on logarithmically decaying  $\epsilon$ -strategy (Blue represents states visited more often and white states rarely or never seen).

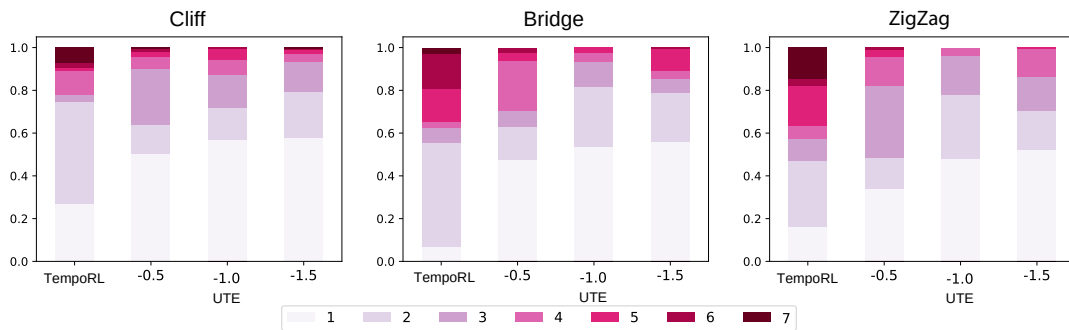


Figure 8: Distribution of extension length for three Lava environments with logarithmically decaying  $\epsilon$  exploration schedule. More red represents more repetitions.

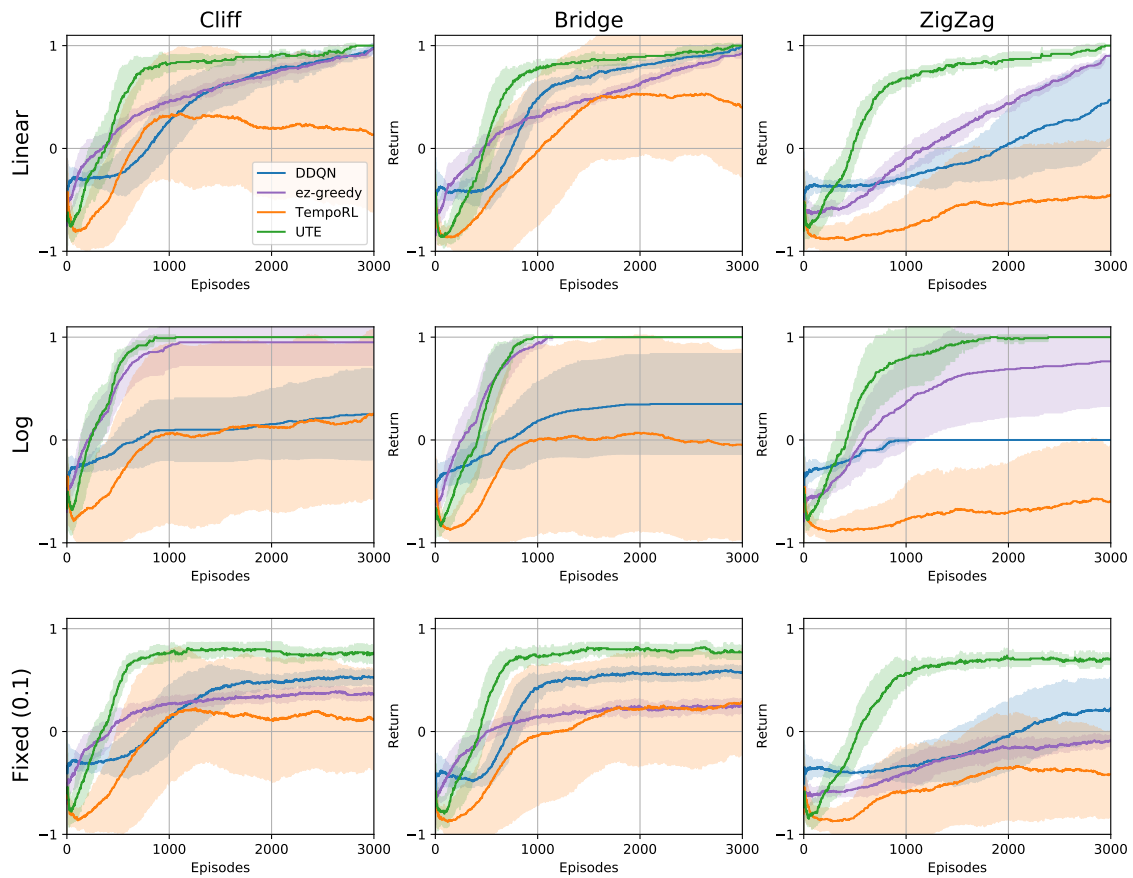


Figure 9: Learning curves across three Lava environments and three different  $\epsilon$ -decaying exploration strategies, comparing UTE with DDQN,  $\epsilon z$ -Greedy and TempoRL. Shaded areas represent the standard deviations over 20 random seeds.

## Atari 2600

**DQN-normalized score.** The DQN-normalized score is defined as

$$score = \frac{\text{agent} - \text{random}}{\text{DQN} - \text{random}}$$

where agent, random, and DQN are the per-game mean rewards over the last 100,000 time steps for the agent, a random policy, and a DDQN respectively. We used this DQN-normalized score to summarize the results across various games.

The results in Table 10 show mean DQN-normalized scores over the last 100,000 time steps of each game. The reason that we use this metric instead of the human-normalized score is that we have only trained the agent for 10 million frames due to limited resources. The agents were not fully trained to be compared with the human scores, so we normalized the score against DDQN. A score below 0 means that the performance is worse than that of random policy while the score greater than 1 indicates it achieves higher performance compared to that of DDQN agent. Overall, our UTE with the best uncertainty parameter performs best compared to other baselines (see Table 10 for more details). UTE achieves a score 81% higher than that of DDQN and 40% higher than TempoRL.

Environment	DDQN	Fixed- $j$	$\epsilon z$ -Greedy	DAR	TempoRL	B-DQN	UTE (1-step)	UTE ( $n$ -step)
Beam Rider	1.00	0.85	2.50	0.05	2.79	1.32	2.41	<b>2.89</b>
Centipede	1.00	0.55	0.82	0.79	1.49	0.63	0.82	<b>1.71</b>
Crazy Climber	1.00	0.70	1.01	0.38	0.93	0.55	1.29	<b>1.56</b>
Freeway	1.00	0.93	0.94	0.83	<b>1.18</b>	1.17	1.17	1.13
Kangaroo	1.00	0.41	1.11	0.56	0.78	0.98	1.07	1.21
Ms Pacman	1.00	0.71	<b>1.21</b>	0.67	0.97	1.02	<b>1.33</b>	1.10
Pong	1.00	0.02	<b>1.02</b>	0.01	0.91	0.98	1.00	1.00
Qbert	1.00	0.48	1.41	0.38	1.08	1.69	1.39	<b>2.09</b>
Riverraid	1.00	0.46	<b>1.29</b>	0.09	1.10	1.15	1.29	1.28
Road Runner	1.00	0.38	1.14	0.26	2.48	1.52	1.51	<b>3.76</b>
Sea Quest	1.00	0.14	1.04	0.12	0.58	0.67	1.00	<b>1.54</b>
Up n Down	1.00	1.13	1.63	0.58	1.23	0.66	1.83	<b>2.05</b>
Average	1.00	0.56	1.28	0.35	1.29	1.03	1.34	<b>1.81</b>

Table 10: DQN-normalized performance averaged over last 100,000 time steps for UTE with the best uncertainty parameter and other baselines. (7 random seeds)

**Per-game Best Parameter.** We applied various kinds of uncertainty parameters to our proposed model from +1.0 to -1.5. As shown in Table 12, the optimal uncertainty parameter varies from environment to environment. In most games, such as *Beam Rider*, *Centipede*, *Crazy Climber*, *Freeway*, *Qbert*, *Road Runner*, *Up n Down*, the uncertainty-averse strategy (negative  $\lambda$ ) exhibits an improvement in averaged rewards over the last 100,000 time steps. Meanwhile, on *Kangaroo*, the exploration-favor strategy (positive  $\lambda$ ) shows better performance.

Table 11 describes that optimal hyperparameter  $\mu$  for  $\epsilon z$ -Greedy also varies from environment to environment. For fair comparison with our algorithm, we used the per-game best  $\mu$  for  $\epsilon z$ -Greedy.

**Multi-arm Bandit for Choosing  $\lambda$ .** To choose  $\lambda$  adaptively, we used multi-armed bandit (MAB) algorithm (Garivier and Moulines 2008) with sliding-window upper confidence bound (UCB) as described in Atari 2600 experiments. Therefore, here we describe the bandit algorithm in detail. The following method is mainly structured by referring to Appendix Section D in Badia et al. (2020).

At each episode  $k \in [K]$ , a  $N$ -armed bandit selects an arm  $A_k$  among the pre-defined set of arms  $\mathcal{A} := \{0, \dots, N - 1\}$  by a policy  $\pi$ . The policy  $\pi$  depends on the sequence of previous histories (actions and rewards). Then, it receives a reward  $R_k(A_k) \in \mathbb{R}$  from the environment.

The objective of an MAB algorithm is to learn a policy  $\pi$  that minimizes the expected regret as follows:

$$\mathbb{E}_\pi \left[ \sum_{k=0}^{K-1} \max_A R_k(A) - R_k(A_k) \right].$$

When reward distribution is stationary, i.e.  $R_k(\cdot) = R(\cdot)$ , the traditional UCB algorithm can be applied. Define the number of

time episodes an arm  $a \in \mathcal{A}$  has been selected in episode  $k$  as:

$$N_k(a) = \sum_{k'=0}^{k-1} \mathbf{1}(A_{k'} = a),$$

where  $\mathbf{1}(A_k = a)$  is an indicator function. We can estimate the empirical mean reward of an arm  $a$  as:

$$\hat{\mu}_k(a) = \frac{1}{N_k(a)} \sum_{k'=0}^{k-1} R_{k'}(a) \mathbf{1}(A_{k'} = a).$$

Then, we select an arm using the UCB algorithm as follows:

$$\begin{cases} \forall 0 \leq k \leq N-1, & A_k = k, \\ \forall N \leq k \leq K-1, & A_k = \operatorname{argmax}_{a \in \mathcal{A}} \hat{\mu}_{k-1}(a) + \beta \sqrt{\frac{\log(k-1)}{N_{k-1}(a)}}. \end{cases}$$

However, if reward distribution is non-stationary, the UCB algorithm cannot be directly applied due to the change in reward distribution. One of the common solutions to the non-stationary case is to use a sliding-window UCB. Let  $\tau \in \mathbb{Z}^+$  be the size of window such that  $\tau < K$ . The number of time episodes an arm  $a \in \mathcal{A}$  has been played in episode  $k$  for a window size  $\tau$  as:

$$N_k^\tau(a) = \sum_{k'=\max(0, k-\tau)}^{k-1} \mathbf{1}(A_{k'} = a). \quad (8)$$

Define the empirical mean reward of an arm  $a$  for a window size  $\tau$  as:

$$\hat{\mu}_k^\tau(a) = \frac{1}{N_k^\tau(a)} \sum_{k'=\max(0, k-\tau)}^{k-1} R_{k'}(a) \mathbf{1}(A_{k'} = a). \quad (9)$$

Then, we select an arm using the sliding window UCB as follows:

$$\begin{cases} \forall 0 \leq k \leq N-1, & A_k = k, \\ \forall N \leq k \leq K-1 & A_k = \operatorname{argmax}_{a \in \mathcal{A}} \hat{\mu}_{k-1}^\tau(a) + \beta \sqrt{\frac{\log(k-1)}{N_{k-1}^\tau(a)}}. \end{cases}$$

Finally, since we use the sliding window UCB with  $\epsilon_{ucb}$ -greedy exploration, our bandit algorithm is as follows:

$$\begin{cases} \forall 0 \leq k \leq N-1, & A_k = k, \\ \forall N \leq k \leq K-1 \text{ and } U_k \geq \epsilon_{ucb}, & A_k = \operatorname{argmax}_{a \in \mathcal{A}} \hat{\mu}_{k-1}^\tau(a) + \beta \sqrt{\frac{\log(k-1)}{N_{k-1}^\tau(a)}}, \\ \forall N \leq k \leq K-1 \text{ and } U_k < \epsilon_{ucb}, & A_k = Y_k, \end{cases}$$

where  $U_k$  is a random variable drawn uniformly from  $[0, 1]$  and  $Y_k$  is a random action sampled uniformly from  $\mathcal{A} = \{0, \dots, N-1\}$ .

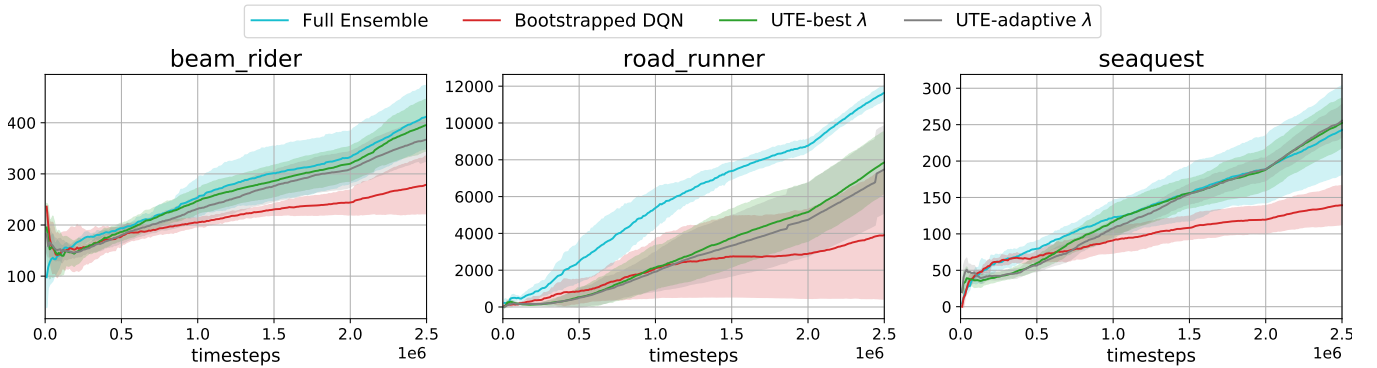


Figure 10: Learning curves of Full Ensemble, B-DQN, UTE with the best uncertainty parameter, and UTE with adaptive uncertainty parameter over 7 random seeds.

In Atari experiments, each arm corresponds to extension length  $\lambda$ . At the beginning of each episode, the bandit algorithm chooses  $\lambda_k$  among the set,  $\lambda_k \in \Lambda := \{+1.0, +0.5, +0.2, 0.0, -0.2, -0.5, -1.0, -1.5\}$ , and gets the feedback of episode rewards  $R_k(\lambda_k)$ . Then, the bandit algorithm update  $N_k^T(a)$  by Eq. (8) and  $\hat{\mu}_k^T(a)$  by Eq. (9).

**Full Ensemble Model.** We additionally evaluated another algorithm, called Full Ensemble. The Full Ensemble is a combination of UTE and B-DQN, which means both action-value functions and option-value functions are estimated by an ensemble method. Figure 10 demonstrates that the Full Ensemble performs similar to or better than others. In an environment where rewards are relatively sparse such as *Road Runner*, Full Ensemble notably outperforms other agents. We did not optimize the uncertainty parameter for Full Ensemble so that there is room for further improvements. The results imply that our method can apply to any base algorithm smoothly.

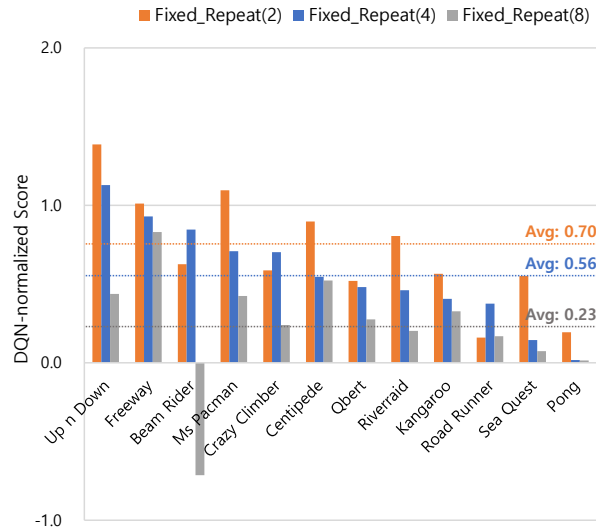


Figure 11: DQN-normalized score for Fixed Repeat with varying fixed  $j$ . (5 random seeds)

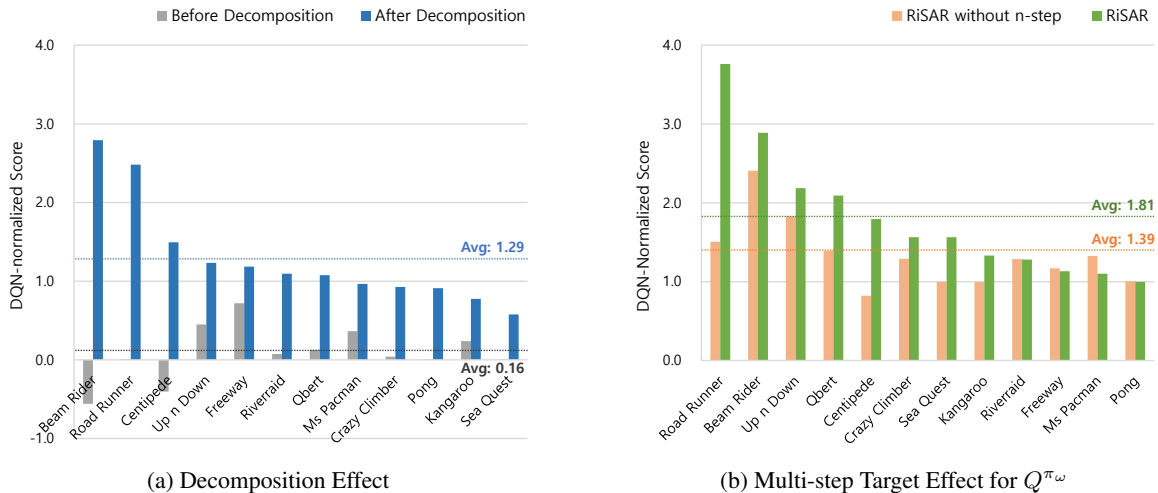


Figure 12: Ablation studies for decomposition effect (left) and  $n$ -step learning effect for action-value function  $Q^{\pi_\omega}$ . The negative score indicates that the policy is worse than a random policy. (5 random seeds)

**Various Fixed Repeat.** Figure 11 shows the performance of Fixed Repeat agents with varying fixed extension length. The fixed extension length affects the granularity of control. The negative score indicates that the performance is worse than a random policy. The result describes that naively repeating the chosen action could degrade the performance in Atari environments. And this tends to get worse as the fixed extension length is increased. However, it still shows a lot worse performance than DQN (score

= 1.0).

**Ablation 1: Decomposition.** Our method formulates joint optimization of the action and the extension length as a two-level optimization problem. The action is selected based on  $Q^{\pi_\omega}$  and then the extension length is selected based on  $\tilde{Q}^{\pi_\omega}$  sequentially. Left of Figure 12a shows the effect of the decomposition. Without decomposition, the size of search space is  $|\mathcal{A}| \times |J|$ , which leads to a catastrophic performance. In some environments such as *Beam Rider* and *Road Runner*, the DQN-normalized scores are negative, which means the agent is worse than a random policy. Overall, We can see that decomposition of action and extension length selection improves the performance significantly.

**Ablation 2: Multi-step Target.** Right of Figure 12b describes the effect of using an  $n$ -step target for  $Q^{\pi_\omega}$ . We compare UTE with  $n$ -step Q-learning to the one without it. This result illustrates that applying  $n$ -step learning is beneficial in most games, which shows a 30.2% improvement (from 1.39 to 1.81) after it has been applied. Especially in games with relatively sparse rewards such as *Road Runner* and *Centipede*, it dramatically enhanced the performance. This is because rewards can be propagated faster using  $n$ -step returns.

Environment	$\epsilon z$ -Greedy ( $\mu$ )				
	1.5	1.75	2.0	2.25	2.5
Beam Rider	331.6	272.9	<b>409.1</b>	261.4	328.9
Centipede	1271.8	1222.6	1080.2	1316.0	<b>1431.7</b>
Crazy Climber	5026.1	4420.0	3128.0	<b>5295.1</b>	4690.9
Freeway	<b>30.8</b>	30.7	25.6	20.5	25.6
Kangaroo	<b>609.1</b>	518.8	604.0	360.0	396.4
Ms Pacman	580.0	551.3	584.5	514.9	<b>597.2</b>
Pong	19.7	18.4	19.8	19.4	<b>19.9</b>
Qbert	<b>392.8</b>	388.6	345.2	264.7	270.6
Riverraid	810.4	835.5	<b>945.6</b>	695.5	738.2
Road Runner	2943.0	2215.2	<b>3733.8</b>	3131.2	848.5
Sea Quest	116.1	<b>214.5</b>	172.6	123.8	119.6
Up n Down	700.6	<b>823.1</b>	669.0	794.8	653.2

Table 11: Average rewards for  $\epsilon z$ -Greedy varying values for hyperparameter  $\mu$  in the Atari 2600 environments. (7 random seeds)

## DDPG Implementation Details and Additional Results

For our base DDPG setup, we used an openly available code from (<https://github.com/sfujim/TD3>) and maintained its default hyperparameters. However, we adjusted the maximum training steps and initial random steps, as detailed in the main paper. While we employ a constant epsilon-greedy exploration for the extension policy for FiGAR and t-DDPG<sup>3</sup>, we refrain from applying epsilon-greedy exploration for UTE-DDPG. This is due to our algorithm already integrating a UCB-style exploration strategy for the extension policy.

Regarding our UTE-DDPG configuration, we employ the algorithm as described in Algorithm 1. The primary distinction lies in substituting normal Q-learning with those specific to DDPG training. For instance, in DDPG, the actor’s exploration policy involves adding exploration noise instead of adhering to an epsilon-greedy policy. Additionally, we again can make use of the base agent’s Q-function to learn the option-value function, as described in Equation (2). Note that our method is **generic** so that it can be applied to any other existing algorithms. This combination of ease-of-use, significantly improved performance, and wide adaptability not only emphasizes its practicality but also underscores the broad applicability of our approach.

Figure 14 depicts the learning curves of various DDPG agents across different maximal extension lengths. The result indicates that UTE-DDPG accelerates learning and achieves superior final rewards compared to other benchmarks, particularly when the maximal extension length is small (e.g.,  $J = 2$  or  $J = 4$ ). Furthermore, our approach showcases remarkable stability, with its efficacy largely unaffected by increasing the maximal extension length. Intriguingly, UTE-DDPG tends to execute action repetitions less frequently than t-DDPG. In this continuous control environments, recklessly repeating actions can deteriorate the performance significantly. Thanks to our *uncertainty-aware* extension, actions are repeated carefully, leading to faster learning.

<sup>3</sup>We followed the description provided by Sharma, Srinivas, and Ravindran (2017) and Biedenkapp et al. (2021)

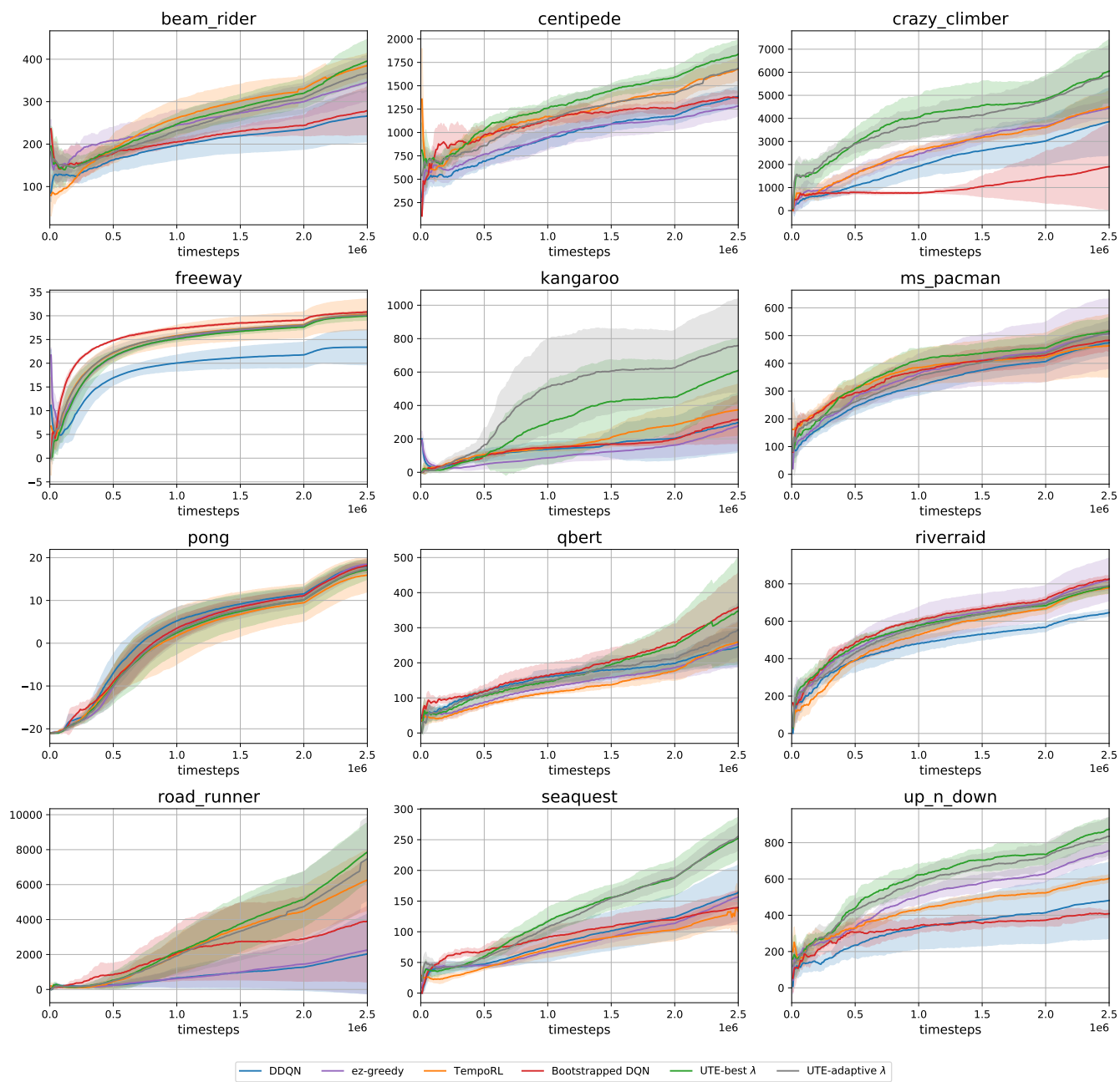


Figure 13: Per-game Atari learning curves for  $\epsilon z$ -Greedy with the best  $\mu$  for zeta distribution, UTE with the best uncertainty parameter, UTE with adaptive uncertainty parameter and the other baselines.(7 random seeds)

Environment	UTE (uncertainty parameter: $\lambda$ )							
	+1.0	+0.5	+0.2	+0.0	-0.2	-0.5	-1.0	-1.5
Beam Rider	384.3 (137.8)	431.6 (162.9)	401.1 (143.3)	425.2 (153.5)	403.1 (127.9)	417.1 (115.4)	<b>439.5</b> (163.0)	414.2 (112.3)
Centipede	1898.2 (889.2)	1327.8 (760.6)	1581.4 (1008.2)	2125.6 (1356.4)	<b>2190.1</b> (1073.0)	1893.6 (954.9)	1605.9 (1167.7)	1377.5 (875.2)
Crazy Climber	5093.2 (4011.6)	4426.2 (3987.4)	6163.6 (5025.2)	5033.9 (2653.9)	6484.8 (4797.2)	<b>8175.6</b> (5790.4)	5198.6 (4049.5)	5220.2 (4751.1)
Freeway	28.6 (3.7)	29.9 (2.0)	27.9 (5.4)	30.5 (1.5)	<b>30.7</b> (1.9)	24.1 (3.9)	25.1 (4.7)	25.0 (6.8)
Kangaroo	555.2 (650.7)	493.3 (515.7)	543.0 (450.3)	661.0 (630.4)	623.3 (630.6)	577.6 (622.6)	718.2 (859.1)	<b>728.5</b> (832.6)
Ms Pacman	446.5 (229.7)	509.6 (256.3)	551.0 (237.5)	545.5 (218.3)	<b>551.6</b> (225.5)	544.1 (249.1)	511.2 (182.2)	540.4 (228.3)
Pong	17.5 (5.9)	18.0 (5.1)	17.1 (5.9)	16.9 (4.5)	<b>19.1</b> (2.5)	16.8 (6.2)	18.4 (4.7)	16.4 (4.6)
Qbert	387.4 (415.8)	400.5 (490.3)	457.4 (461.3)	399.2 (461.9)	297.2 (302.7)	417.1 (441.0)	<b>582.5</b> (558.7)	459.1 (499.7)
Riverraid	<b>938.0</b> (388.8)	828.6 (339.6)	823.3 (363.0)	922.1 (418.0)	880.3 (341.0)	909.8 (350.1)	863.1 (354.8)	795.8 (310.5)
Road Runner	10051.5 (4107.8)	10853.3 (5789.4)	10712.7 (3290.1)	9788.2 (4054.3)	9019.5 (4469.1)	<b>12323.2</b> (4177.1)	6638.6 (3602.0)	5763.6 (4681.0)
Sea Quest	260.3 (126.7)	301.0 (162.6)	290.4 (154.4)	308.5 (150.8)	<b>313.4</b> (141.1)	282.4 (164.7)	250.9 (162.0)	226.8 (125.4)
Up n Down	1012.7 (613.6)	999.6 (504.3)	865.8 (451.2)	912.1 (611.0)	990.3 (532.0)	972.5 (530.2)	<b>1072.8</b> (664.0)	1039.6 (573.0)

Table 12: Average rewards and standard deviations (numbers in bracket) over the last 100,000 time steps for different uncertainty parameter of our proposed method. (7 random seeds)

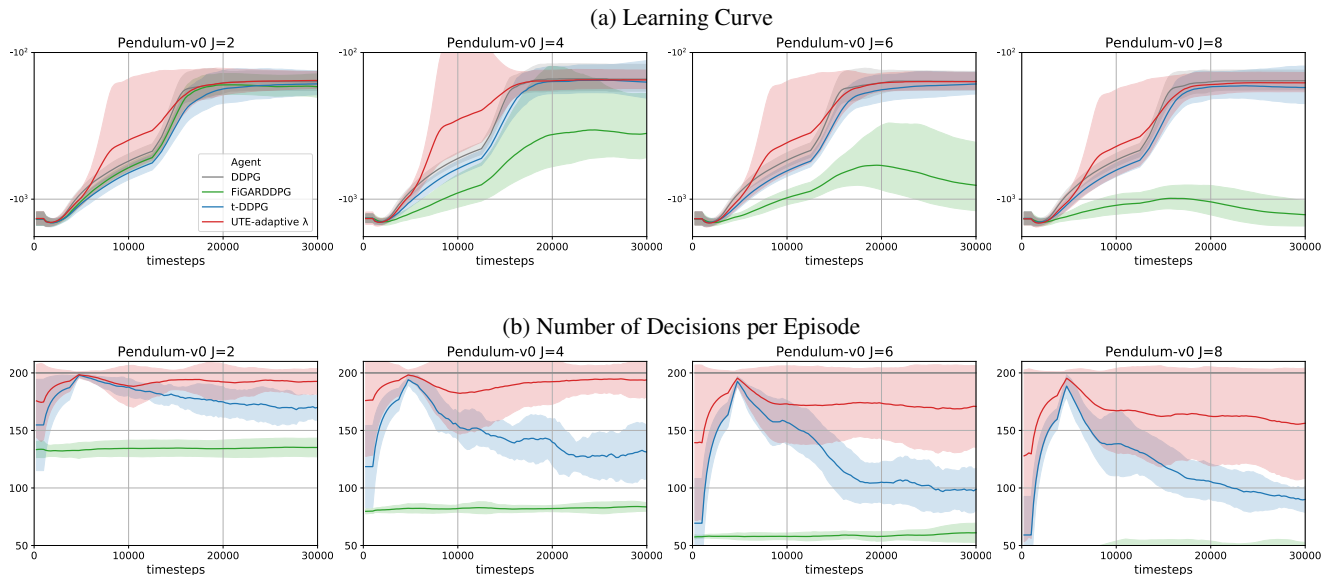


Figure 14: Learning curves for DDPG, FiGAR,  $\tau$ -DDPG, UTE with adaptive  $\lambda$  on Pendulum-v0.  $J$  represents the maximal extension length utilized during the training of UTE with adaptive  $\lambda$ ,  $\tau$ -DDPG, and FiGAR. Solid lines represent the average, while the shaded regions reflect the standard deviation across 20 trials. Images in the top row (a) display the rewards obtained, while those in the bottom row (b) illustrate the steps and decisions needed for each evaluation rollout.

Environment	DDQN	Fixed- $j$	$\epsilon$ -Greedy	DAR	TempoRL	B-DQN	UTE		
							1-step	$n$ -step	Adaptive $\lambda$
Beam Rider	290.1	277.9	409.9	177.7	431.9	315.6	414.4	<b>439.5</b>	423.9
	(101.5)	(109.9)	(124.0)	(73.3)	(140.4)	(131.1)	(141.1)	(163.0)	(158.5)
Centipede	1574.7	1222.8	1431.7	1410.3	1958.0	1285.2	1437.1	<b>2190.1</b>	1829.9
	(1044.6)	(840.8)	(1169.1)	(982.8)	(1166.4)	(867.2)	(887.2)	(1073.0)	(969.6)
Crazy Climber	5265.8	3731.1	5295.1	2059.1	4885.5	2961.6	6761.9	<b>8175.6</b>	7046.3
	(4063.4)	(2997.2)	(3609.7)	(1225.1)	(3378.3)	(3080.0)	(5061.9)	(5790.4)	(5350.0)
Freeway	27.1	25.2	30.8	22.5	<b>32.1</b>	31.7	31.7	30.7	30.8
	(4.6)	(3.1)	(1.3)	(2.9)	(1.0)	(1.1)	(1.2)	(1.9)	(1.7)
Kangaroo	547.2	222.2	609.1	305.5	424.2	534.8	586.4	<b>728.5</b>	661.0
	(764.9)	(247.9)	(880.1)	(340.6)	(282.0)	(467.4)	(753.5)	(832.6)	(613.5)
Ms Pacman	509.8	388.8	597.2	371.3	495.6	516.1	<b>645.6</b>	551.6	537.6
	(204.6)	(201.6)	(261.5)	(166.5)	(245.1)	(206.5)	(267.1)	(225.5)	(263.8)
Pong	19.2	-20.3	<b>19.9</b>	-20.6	15.6	18.3	19.4	19.1	19.5
	(4.8)	(0.9)	(1.8)	(0.6)	(7.7)	(3.6)	(1.8)	(2.5)	(2.3)
Qbert	278.3	133.8	392.8	104.7	299.7	470.8	387.3	<b>582.5</b>	581.4
	(312.9)	(267.9)	(438.3)	(70.8)	(349.8)	(489.5)	(423.1)	(558.7)	(602.5)
Riverraid	740.5	360.9	<b>945.6</b>	102.8	807.7	843.8	942.2	938.0	890.5
	(291.9)	(231.6)	(457.9)	(66.0)	(354.7)	(407.2)	(319.3)	(388.8)	(330.7)
Road Runner	3277.0	1230.3	3733.8	845.5	8131.5	4976.8	4935.6	<b>12323.2</b>	10353.3
	(4470.3)	(1640.9)	(4716.5)	(791.9)	(4099.3)	(6032.6)	(5206.4)	(4177.1)	(3283.3)
Sea Quest	207.6	47.0	214.5	42.8	128.2	145.1	206.9	313.4	<b>320.3</b>
	(124.5)	(26.2)	(85.6)	(33.9)	(55.5)	(64.5)	(92.4)	(141.1)	(159.4)
Up n Down	536.4	594.8	823.1	348.7	641.5	383.2	911.5	<b>1072.8</b>	990.4
	(361.5)	(324.6)	(320.0)	(227.0)	(428.6)	(242.8)	(476.7)	(664.0)	(707.5)

Table 13: Average rewards and standard deviations (numbers in bracket) over the last 100,000 time steps over Atari environments.